

1 **ADVANCING GLOBAL AEROSOL SIMULATIONS WITH SIZE-**
2 **SEGREGATED ANTHROPOGENIC PARTICLE NUMBER EMISSIONS**

3 FILIPPO XAUSA¹, PAULI PAASONEN^{1,5}, RISTO MAKKONEN¹, MIKHAIL
4 ARSHINOV², AIJUN DING³, HUGO DENIER VAN DER GON⁴, VELI-MATTI
5 KERMINEN¹, MARKKU KULMALA¹

6 ¹ *Division of Atmospheric Sciences, Department of Physics, University of*
7 *Helsinki.*

8 ² *Institute of Atmospheric Optics, SB RAS, 634055, Tomsk, Russia.*

9 ³ *Joint International Research Laboratory of Atmospheric and Earth System*
10 *Sciences, School of Atmospheric Sciences, Nanjing University, Nanjing*
11 *210023, China.*

12 ⁴ *TNO, Department of Climate, Air and Sustainability, Utrecht, the*
13 *Netherlands.*

14 ⁵ *International Institute for Applied Systems Analysis (IIASA), Laxenburg,*
15 *Austria*

16
17
18 Keywords: AEROSOL, NUMBER SIZE DISTRIBUTION, GAINS, GLOBAL CLIMATE
19 MODEL

20
21 ABSTRACT

22 Climate models are important tools that are used for generating climate
23 change projections, in which aerosol-climate interactions are one of the main
24 sources of uncertainties. In order to quantify aerosol-radiation and aerosol-
25 cloud interactions, detailed input of anthropogenic aerosol number emissions
26 is necessary. However, the anthropogenic aerosol number emissions are
27 usually converted from the corresponding mass emissions in precompiled
28 emission inventories through a very simplistic method depending uniquely
29 on chemical composition, particle size and density, which are defined for a
30 few very wide main source sectors. In this work, the anthropogenic particle
31 number emissions converted from the AeroCom mass in the ECHAM-HAM

32 climate model were replaced with the recently-formulated number emissions
33 from the Greenhouse Gas and Air Pollution Interactions and Synergies
34 (GAINS)-model. In the GAINS model the emission number size distributions
35 vary, for example, with respect to the fuel and technology. Special attention
36 was paid to accumulation mode particles (particle diameter $d_p > 100$ nm)
37 because of (i) their capability of acting as cloud condensation nuclei (CCN),
38 thus forming cloud droplets and affecting Earth's radiation budget, and (ii)
39 their dominant role in forming the coagulation sink and thus limiting the
40 concentration of sub-100 nanometers particles. In addition, the estimates of
41 anthropogenic CCN formation, and thus the forcing from aerosol-climate
42 interactions are expected to be affected. Analysis of global particle number
43 concentrations and size distributions reveal that GAINS implementation
44 increases CCN concentration compared with AeroCom, with regional
45 enhancement factors reaching values as high as 10. A comparison between
46 modeled and observed concentrations shows that the increase in number
47 concentration for accumulation mode particle agrees well with
48 measurements, but it leads to a consistent underestimation of both
49 nucleation mode and Aitken mode ($d_p < 100$ nm) particle number
50 concentrations. This suggests that revisions are needed in the new particle
51 formation and growth schemes currently applied in global modeling
52 frameworks.

53

54 1 Introduction

55 In recent years, the link between anthropogenic aerosol particle and climate
56 change has been a subject of several studies (e.g. Baker et al., 2015; Zhang
57 et al., 2016). Anthropogenic aerosol particles play an important role in the
58 global climate system via aerosol-radiation and aerosol-cloud interactions by
59 scattering and absorbing solar radiation and by acting as cloud condensation
60 or ice nuclei, thereby changing many cloud properties (Boucher et al., 2013).
61 The global and regional radiative effects of aerosol particles depend on the
62 spatial and temporal distribution of the aerosol number size distribution and
63 chemical composition (Lohmann and Feichter, 2005; Schulz et al., 2006;
64 Forster et al., 2007; Stier et al., 2007).

65 While anthropogenic primary emissions introduce cloud condensation nuclei
66 (CCN) directly into the atmosphere, a significant fraction of the global CCN
67 population is likely be formed through condensation of organic and other low-

68 volatility vapors onto ultra-fine particles (particle diameter $d_p < 100$ nm) in
69 the atmosphere (Spracklen et al., 2008; Merikanto et al., 2009; Kerminen et
70 al., 2012; Paasonen et al., 2013). Aerosol particles and their precursor vapors
71 are emitted from both biogenic and anthropogenic sources, in addition to
72 which they may also result from interactions between biogenic and
73 anthropogenic emissions (Spracklen et al., 2011; Shilling et al., 2013). The
74 increasing number concentration of accumulation mode particles decreases
75 the formation and growth of smaller particles by increasing the sink for
76 condensing vapor molecules, termed the condensation sink (CS, Kulmala et
77 al., 2001), and by increasing the coagulation sink for small freshly-formed
78 particles. Hence, the number concentration of accumulation mode particles
79 from primary emissions affects secondary aerosol formation. The effects of
80 these physical processes on future aerosol climate forcing requires
81 application of detailed aerosol microphysical schemes in global climate
82 models. Furthermore, the global uncertainty in CCN is highly sensitive to the
83 assumed emission size distribution (Lee et al., 2013).

84 The global aerosol climate model ECHAM-HAM (Stier et al., 2005; Zhang et
85 al., 2012) is a useful tool that aims at increasing our understanding of
86 aerosol-climate interactions. Past simulations performed with the ECHAM-
87 HAM include an extensive analysis of particle nucleation (Makkonen et al.,
88 2009, 2014; Kazil et al., 2010), aerosol properties (Roelofs et al., 2010), and
89 emission data set implementation (Zhang et al., 2012). Although the ECHAM-
90 HAM has a detailed microphysics module for describing the aerosol size
91 distribution (Vignati et al., 2004), previous studies have not included an
92 exhaustive module for the model-input particle number size distribution. Also
93 in other climate models, the mass-only aerosol input is a commonly applied
94 setting (Jones et al., 2007; Shindell et al., 2007). The main reason behind this
95 resides in the structure of the input data rather than in the models
96 themselves.

97 One of the input emission inventories that has been widely used in ECHAM-
98 HAM simulations, as well as in other Earth System Models (Pozzoli et al.,
99 2011; Makkonen et al., 2009, 2012; Tonttila et al., 2015), is the Aerosol Inter
100 Comparison data set, AeroCom (Dentener et al., 2006), developed for the
101 purpose of conducting improved simulations of aerosol-climate interactions
102 (Samset et al., 2014). However, the AeroCom emission inventory does not
103 include a specific framework for particle number emissions. Hence, the input
104 particle number emissions used in the simulations with AeroCom are

105 estimated from the particle mass emissions by the ECHAM-HAM during the
106 initialization routine. In more detail, the estimation of number emissions
107 consists of a simplistic multiplication of the given AeroCom mass emissions
108 by a mass-to-number conversion factor. Each conversion factor that is
109 applied for building the log-normal distribution is calculated by assuming
110 that the mass emissions for each main source sector are distributed to
111 predefined modes according to predefined densities, geometric mean radii
112 and standard deviations, as described by Vignati et al., (2004) and Stier et
113 al., (2005). This simplistic mass-to-number conversion factor does not
114 represent the relationship between the particle mass and number size
115 distributions in a realistic way, because such framework does not take into
116 account the variation of emitted particle number size distributions from
117 different emitting sources. The AeroCom inventory includes anthropogenic
118 activities, from which the mass-to-number converted emissions are split into
119 half between the Aitken and accumulation modes, and finally converted into
120 log-normal modes. However, the recently-developed inventories allow for
121 global aerosol simulations with a more detailed aerosol emission size
122 distribution (Paasonen et al., 2016) with the GAINS emission scenario model
123 (Greenhouse gas - Air pollution INteractions and Synergies; Cofala et al.,
124 2009; Amann et al., 2011). GAINS data are organized into more detailed
125 anthropogenic sources than AeroCom, with different particle number
126 emissions and size distributions related to different fuels and technologies.

127 In this work, we first develop a novel module for anthropogenic particle
128 number emissions in Earth System Models. Our experiment, performed with
129 ECHAM-HAM, consists of replacing the mass-to-number converted
130 anthropogenic AeroCom aerosol emissions with number emissions from the
131 GAINS-model. In more detail, the implementation of GAINS data set is
132 performed by using ECHAM-HAM default assumptions for AeroCom data set
133 implementation. This study has a dual target: first, it aims at improving the
134 ECHAM-HAM capability for estimating particle number concentrations, with a
135 special focus on accumulation mode particles, and second, it investigates the
136 feasibility of using the GAINS model for global climate modeling studies by
137 running the ECHAM-HAM with both AeroCom and GAINS data sets. We
138 present a comparison between the novel GAINS implementation and the
139 default implementation of AeroCom in ECHAM-HAM, including modeled
140 particle number concentrations and size distributions, as well as modeled
141 CCN number concentrations. Finally, we compare the modeled number size
142 distributions with observations in different environments around the world.

143

144 2 Materials and methods

145 2.1 The ECHAM5.5-HAM2 climate model

146 We used the global aerosol climate model ECHAM5.5-HAM2 (Stier et al.,
147 2005; Zhang et al., 2012) with the M7 microphysics module (Vignati et al.,
148 2004). The M7 describes the aerosol number size distribution with seven log-
149 normal modes, in which the Aitken, accumulation and coarse modes are
150 present in both the soluble and insoluble phases, while the nucleation mode
151 is present only as the soluble mode. The compounds modeled in our
152 simulations are black carbon (BC), organic carbon (OC), sulfate (SO₄), dust
153 and sea salt. The emission module used in ECHAM-HAM reads data for
154 anthropogenic, biogenic, wildfire, volcanic, agricultural emissions, secondary
155 organic aerosols (SOA) and shipping sources. In our experiments, we
156 modified only the part of the ECHAM-HAM source code that handles the
157 anthropogenic emissions. The model has a horizontal gaussian grid (192×96)
158 with a grid box size of ~200×200 km at the equator, and a vertical resolution
159 of 31 hybrid sigma layers.

160

161 2.1.1 Aerosol microphysics

162 The version of ECHAM-HAM used in this work includes nucleation,
163 condensation and coagulation modules. Previous studies have shown that
164 the implementation of an activation-type nucleation improves particle
165 number concentration estimations in modeling (Spracklen et al., 2010;
166 Makkonen et al., 2012). In our experiment, we coupled a binary sulphuric
167 acid-water nucleation scheme (Vehkamäki et al., 2002) with an activation-
168 nucleation scheme described by Paasonen et al., (2010, Eq. 10), in which the
169 nucleation rate (J) is a function of the activation coefficient and sulphuric acid
170 concentration, expressed as

$$171 \quad J = 1.7 \times 10^{-6} s^{-1} * [H_2SO_4] \quad (1)$$

172 The settings of our simulations included a specific module for SOA formation.
173 Here, we modeled the SOA formation with both kinetic condensation onto a
174 Fuchs-corrected surface area (CS) and partitioning according to a preexisting
175 organic mass (Riipinen et al., 2011; Jokinen et al., 2015). This SOA module

176 includes three biogenic volatile organic compound (BVOC) tracers: isoprene,
177 endocyclic monoterpenes and other monoterpenes, each having monthly
178 resolutions for emissions. We did not use any nucleation scheme for organic
179 vapors, because the simple activation-type nucleation, while not accurate for
180 individual sites, describes the nucleation in different environments
181 reasonably well (Paasonen et al., 2010). The particle growth from nucleation
182 size to the d_p of 3 nm was calculated according to Kerminen and Kulmala
183 (2002), considering both sulfuric acid and organic vapour condensation. More
184 details can be found in Makkonen et al. (2012).

185

186 2.1.2 Natural emissions

187 BVOC emissions were implemented using the MEGAN2 (Guenther et al.,
188 2006) model. MEGAN2 estimates biogenic emissions for about 150
189 compounds from different ecosystems, paying a particular attention to
190 monoterpenes. This framework takes into account several factors that
191 influence BVOC emissions, including the leaf age, soil moisture and light
192 environment. MEGAN2 was run offline and its output data were used for the
193 ECHAM-HAM input initialization.

194 All non-anthropogenic emissions, such as volcanic emissions, dimethyl-
195 sulfide (DMS, Kloster et al., 2006) emitted by the sea and dust, were taken
196 from AeroCom in both simulations. All emission data, excluding SOA
197 precursors, DMS emissions and wildfire, were input as annual-averages. As a
198 result, the seasonality in concentrations of anthropogenic compounds is
199 mostly due to the nudged meteorology.

200

201 2.1.3 Anthropogenic emissions

202 The first simulation was performed with the ECHAM-HAM default
203 implementation of anthropogenic emissions from AeroCom data set for year
204 2000. The AeroCom emissions taken by the ECHAM-HAM are provided by
205 mass as $\text{kg m}^{-2} \text{s}^{-1}$ with a chemical differentiation that includes BC, OC and
206 SO_4 , and a bi-level vertical distribution (2-zL) that consists of two surface
207 layers: a lower level below 100 meters above the sea level for emissions
208 from transportation and domestic combustion, and a higher level for
209 industrial activities whose emissions reach altitudes higher than 100 meters.

210 While BC does not require preprocessing during the simulation, input
 211 emissions of OC and SO₄ undergo a further conversion during the
 212 initialization routine: OC mass is converted into primary organic matter
 213 (POM) mass with a multiplying factor 1.4 (Turpin et al., 2000; Kupiainen and
 214 Klimont, 2007), and emissions containing sulfur (S) are input as both sulfur
 215 dioxide (SO₂) and SO₄. The primary SO₄ particle fraction is estimated as 2.5%
 216 of gaseous SO₂, as described by Dentener et al. (2006). The masses of BC
 217 and POM are uniquely treated as Aitken mode particles ($d_p = 10-100$ nm).
 218 The mass of SO₄ is divided between the Aitken mode, accumulation mode (d_p
 219 = 100-1000 nm) and coarse mode ($d_p > 1$ μm) through a rough estimation:
 220 the lower-surface-level SO₄ is split equally between the Aitken mode and
 221 accumulation mode, whereas the higher-surface-level SO₄ is split equally
 222 between the accumulation mode and coarse mode. The mass is then
 223 converted by the model into a particle number size distribution. The mass-to-
 224 number flux factors, expressed as $m2n$ in Figure 1, are embedded in the
 225 emission-reading routine. The number of particles is calculated through the
 226 generic function

$$227 \quad N = M/m \quad , \quad (2)$$

228 where M is the mass of given emissions and m is the average mass
 229 estimated for a single particle. The particle mass m in Eq. (2) is extended in
 230 the model according to the Hatch-Choate conversion equations (Hinds,
 231 1982), in which the density, count median radius and standard deviation are
 232 predefined for each chemical compound and size mode, as described by
 233 Stier et al. (2005). The emission count median radius is fixed at 30 nm and
 234 75 nm for the Aitken mode and accumulation mode, respectively, and the
 235 standard deviation is set to 1.59 for all the modes except the coarse mode
 236 for which it is 2.0. The species density is set to 1841 $kg\ m^{-3}$ for SO₄ (input in
 237 the model as H₂SO₄) and 2000 $kg\ m^{-3}$ for BC and OC. Altogether, these
 238 parameters differentiate the species according to their chemistry and
 239 solubility. The number flux conversion is therefore expressed as

$$241 \quad N = \frac{M}{\frac{4}{3} \cdot \pi \cdot \rho_i \cdot (\text{cmr}_{jk} \cdot \text{cmr} 2 \text{ ram}_{jk})^3} \quad , \quad (3)$$

242 where ρ is the density of a determined chemical compound i , and the
 243 expression in brackets is the mean radius of a particle with certain solubility j

244 and size mode k . The quantity cmr is the predefined count median radius as
245 it is expressed in the model code, while $cmr2ram$ is a conversion factor that
246 multiplies cmr in order to estimate the radius of average mass. The $cmr2ram$
247 factor depends uniquely on the standard deviation of the log-normal particle
248 number distribution.

249

250 2.2 Emission scenario model GAINS

251 The GAINS (Greenhouse gas - Air pollution Interactions and Synergies) model
252 is an integrated assessment model developed at IIASA (International Institute
253 for Applied Systems Analysis) in Laxenburg, Austria (Amann et al, 2011). In
254 order to calculate the emissions related to specific anthropogenic source
255 sectors, it combines the information of the annual level of the anthropogenic
256 activities, amounts of different fuels consumed for combustion activities,
257 shares of different emission abatement technologies, and emission factors
258 for different activity-fuel-technology-combinations.

259 The GAINS scenarios include information on the annual activity levels and
260 shares of emission control technologies for nearly 170 regions, being
261 countries or parts or groups of countries, in five-year intervals from 1990 to
262 2050. The activity levels are based on national and international statistics,
263 latter available from International Energy Agency (IEA), Organisation for
264 Economic Co-operation and Development (OECD), United Nations (UN) and
265 Food and Agriculture Organization of the United Nations (FAO) and Eurostat,
266 and the shares of control technologies are derived from national and
267 international information on the related legislation, discussion with national
268 experts and scientific publications. The emission factors for all combinations
269 of source sectors, fuels and technologies are determined from the scientific
270 publications or measurement databases. For detailed description of sources
271 and methods to derive underlying particulate matter emissions see Klimont
272 et al. (2016).

273 The particle number emission factors with the related number size
274 distributions were recently implemented to GAINS (Paasonen et al., 2016).
275 This implementation allowed for detailed assessment of particle number
276 emissions with more than 1000 measures controlling emissions in each of
277 the close to 170 regions, and in internally consistent manner with emissions
278 of other air pollutants and greenhouse gases. The GAINS particle number

279 emissions are known to be subject to uncertainties, especially in terms of
280 nucleation mode emissions, but the major particle number sources, such as
281 road transport and residential combustion, are reasonably well represented
282 down to the control technology level. The determination of emission factors
283 for particle number emissions and particle size distributions is based on the
284 European particle number emission inventory developed by TNO (Denier van
285 der Gon et al., 2009, 2010).

286 In this study, we applied the gridded particle number emissions for year
287 2010 (Paasonen et al., 2016), in which the activity measures and emission
288 abatement technology shares are based on the 'ECLIPSE version 5' dataset
289 (Klimont et al., 2016) developed within the EU FP7 ECLIPSE project (Stohl et
290 al., 2015). The gridded dataset and their brief characterization is freely
291 available from the IIASA website:

292 <http://www.iiasa.ac.at/web/home/research/researchPrograms/air/PN.html>.

293

294 2.3 GAINS implementation in M7

295 In the second simulation, the sub-module that converts the input mass to the
296 number flux described in Eqs. (2-3) was switched off and we implemented
297 the recently-developed 2010 GAINS anthropogenic emissions (Paasonen et
298 al., 2016; see also section 2.1.2). The emission sectors considered for our
299 experiment included the energy production, flares, industrial combustion and
300 processes, transportation, waste combustion and domestic/commercial
301 combustion. A detailed description of the sectors and emission factors is
302 presented in Paasonen et al. (2016).

303 The number size distribution data provided by GAINS are organized into nine
304 size bins with a geometric diameter ranging from 3 nm to 1000 nm.
305 However, in this study we implemented the GAINS data for the Aitken mode
306 and accumulation mode only ($d_p = 10-1000$ nm), so that the particle number
307 implementation was consistent with the AeroCom simulation which lacked
308 the nucleation mode conversion factor in the source code aerosol module.
309 The conversion of GAINS emissions from sectional to modal size distribution
310 is performed by taking the total particle number in the defined Aitken and
311 accumulation modes and emitting them with the same median radii as for
312 the ECHAM-HAM default assumptions (Stier et al., 2005). It should be noted
313 that the ratio of Aitken to accumulation mode emissions can vary between

314 grid cells in both AeroCom and GAINS. In AeroCom this variation is due to
315 different mass-to-number conversion factors for different emission sectors,
316 but in GAINS the size distributions are different also for different technologies
317 and fuels within the emission sectors (e.g. different vehicle technologies,
318 different domestic stove categories, diesel fuels with different sulfur
319 contents, different coal types). This choice of implementation does not fully
320 exploit all the information available in the GAINS size distribution, because
321 the default ECHAM-HAM emission module does not allow the emission
322 diameter to vary on a per-gridbox basis. Although it would be possible to
323 upgrade the ECHAM-HAM in this sense, it would be quite laborious and
324 beyond the scope of our study. It should be noted that the ratio of Aitken to
325 accumulation mode emissions can vary between grid cells in both AeroCom
326 and GAINS. In AeroCom this variation is due to different mass-to-number
327 conversion factors for different emission sectors, but in GAINS the size
328 distributions are different also for different technologies and fuels within the
329 emission sectors (e.g. different vehicle technologies, different domestic stove
330 categories, diesel fuels with different sulfur contents, different coal types).

331 In the GAINS simulation we kept the AeroCom data for the gas phase sulfur
332 and coarse SO_4 in order to identify the global impact of GAINS
333 implementation on submicron particles. Furthermore, we used the same bi-
334 level 2-zL scheme as for the SO_4 vertical distribution in AeroCom: emissions
335 from the transportation, agriculture fires, waste combustion and domestic
336 combustion were put into the lower level (<100 m a.s.l.), whereas the
337 energy, flares, industry and power plant sectors of GAINS were implemented
338 into the higher level (>100 m a.s.l.).

339 GAINS provides the number emission data without chemical speciation and
340 vertical distribution (see Table 1), and separately mass emissions of particle
341 mass, particulate OC and BC, as well as gaseous pollutants, including SO_2 .
342 However, distributing the different compounds between the different number
343 sizes bins is non-trivial task which requires, in order to be properly
344 completed, elaboration of the proper GAINS model, not only the
345 implementation. For this reason, we decided to use the default ECHAM-HAM
346 particle composition from AeroCom in this study and leave the
347 implementation of GAINS chemical composition for future studies. We
348 followed a series of steps in order to partition the GAINS raw data into BC,
349 POM and SO_4 in a consistent format for the model. Table 1 and Figure 1
350 visually illustrate the implementation framework. In more detail, we (I) off-

351 line converted AeroCom mass into number using ECHAM-HAM factors, (II)
352 estimated the chemical species fraction among the respective Aitken mode
353 and accumulation mode in AeroCom numbers, (III) applied such fractions to
354 the total Aitken mode and accumulation mode particle numbers in the GAINS
355 to have the correspondent BC, OC and SO₄ repartition, and finally, IV) used
356 the mass-to-number factors used in (I) to estimate the speciated GAINS
357 mass.

358 Shipping emissions are embedded in the AeroCom data set, but not included
359 in GAINS. In our experiment, we masked out the AeroCom shipping emissions
360 with a land-sea mask produced by applying Climate Data Operator (CDO) to
361 the AeroCom. Hence, shipping emissions were not taken into consideration.

362

363 2.4 Simulation setup

364 Our experiment consisted of two one-year simulations, using identical model
365 settings but different data set for anthropogenic sources: AeroCom and
366 GAINS (see Sect. 2.3). The experiment run was set to start indicatively on
367 October 1, 2009 and end on December 31, 2010 with a three-month spin-up
368 period and one-hour time resolution for the output. The modeled data for our
369 analysis were collected from January 1, 2010 to December 31, 2010. The
370 model was nudged against 2010 ECMWF ERA-Interim (Berrisford et al., 2011)
371 observed meteorology data in order to reduce noise in model estimations
372 and to increase the statistical significance of the eventual anthropogenic
373 aerosol perturbation signal (Kooperman et al., 2012).

374

375 2.5 Comparison with observation

376 Our study focused on particle number concentration and size distributions
377 along with CCN concentrations at the supersaturations of 0.2% (CCN0.2) and
378 1.0% (CCN1.0). We compared the modeled particle number concentrations
379 and size distributions against observations collected from 11 sites around the
380 world. A detailed description of the observation data is illustrated in Table 2.
381 The modeled data extracted from all sites were averaged over the year and
382 plotted against observations to investigate the overall model performance. In
383 addition to visual comparison between the modeled and observed
384 concentrations, we calculated the relative bias as

385
$$\exp\left(\left|\log\left(\frac{model}{observation}\right)\right|\right), \quad (4)$$

386 This relative bias returns the factor, larger than 1, with which the model
387 under or over predicts the observation.

388 The particle number concentration and mean particle radius of the whole
389 output data were used for plotting the number distributions from 6 of the 11
390 original sites, which were chosen to represent areas with a strong presence
391 of anthropogenic emissions (Nanjing, Sao Paulo and Tomsk) as well as areas
392 dominated by biogenic emissions (Hyytiälä, K-Pusztta and Värriö). In both
393 annual-average and number distribution comparisons, the modeled layer
394 closest to Earth's surface was chosen for analysis. Modeled CCN
395 concentrations were studied by comparing simulations with AeroCom
396 emissions against those from GAINS emissions for both CCN0.2 and CCN1.0.
397 CCN concentrations were extracted and averaged from the lowest three
398 model layers in order to reduce background noise in mapping the global
399 concentrations. Due to the coarse grid size and inhomogeneous sources
400 around measurement sites, the evaluation against observations is not
401 expected to yield one-to-one validation of aerosol concentrations (Schutgens
402 et al., 2016).

403

404 3 Results and discussion

405 Here we show the comparison between AeroCom and GAINS implementation
406 before (emissions, section 3.1) and after (atmospheric concentrations,
407 sections 3.2 and 3.3) running the ECHAM-HAM model. Our experiment was
408 performed with the same model settings in both simulations and it was
409 nudged against meteorology data. As a result, our analysis focused merely
410 on the differences between the particle number emissions of the two data
411 sets and their different effects on modeled particle concentrations. In the
412 following sections, we will first show the difference between AeroCom and
413 GAINS in terms of input emissions, after which we will compare the model-
414 simulated particle number concentrations and size distributions with
415 observational data. Finally, we will assess the effect of the GAINS
416 implementation on global CCN concentrations.

417

418 3.1 Differences in particle number emissions

419 In this section, we present a preliminary assessment of input emissions to
420 illustrate the main differences between the two gridded data sets before
421 starting the simulation. Table 3 shows global emissions and their ratios
422 between GAINS and AeroCom for the whole domain. When the emissions
423 were globally averaged (R_{tot}), GAINS showed higher total number emissions
424 by a factor of 2.2. However, when looking at individual grid cells, the total
425 particle number emission ratios between AeroCom and GAINS had a large
426 spatial variability (Figure 2), even though the median value of this ratio was
427 very close to one (see R_{grid} in Table 3). Figure 3 shows the spatial distribution
428 of both emissions data sets. Globally, the Aitken to accumulation mode
429 particle emission ratio was about two orders of magnitude in AeroCom
430 emissions, while being less than a factor four in GAINS emission. The
431 averaged emission ratios demonstrate that accumulation mode emissions
432 play a critical role in the GAINS implementation, with both R_{tot} and R_{grid} ratios
433 increasing dramatically compared with AeroCom. The averaged Aitken mode
434 particle emissions from GAINS did not show a similar increase, and the R_{grid}
435 median value was even lower than that in the AeroCom emissions. The R_{tot}
436 and R_{grid} ratios of Aitken mode emissions were 1.7 and 0.7, respectively. This
437 difference shows that the Aitken mode particle emissions are quantitatively
438 higher in GAINS than in AeroCom when their geographical distribution
439 differences are not taken into account. However, when the data sets were
440 compared by confronting each grid cell one by one, AeroCom emissions were
441 higher than GAINS emissions in a prevalent area of the global domain.

442 It should be noted that in the ECHAM-HAM assumptions made for the
443 AeroCom emissions, fossil fuel and biofuel emissions are implemented in the
444 Aitken mode only. In more detail, all BC emissions from AeroCom are
445 implemented in the M7 module as insoluble Aitken mode particles, which are
446 converted to soluble particles after sulfate condensation. In GAINS, the
447 particles estimated to contain BC are distributed into particle size bins at
448 around 100 nm (Paasonen et al., 2016). The difference between the
449 diameters of emissions from fossil fuel and biofuel combustion is the major
450 reason behind the differences in accumulation mode emissions and
451 concentrations.

452 The differences in Aitken and accumulation mode emissions between GAINS
453 and AeroCom implementations originate from three main differences

454 between the emission data bases. Firstly, the GAINS emission factors,
455 especially in traffic and residential combustion sectors, are directly based on
456 literature or databases of particle number emissions, whereas in AeroCom
457 the number emissions are converted from mass emissions. This causes
458 differences in the relative shares of different source sectors in the emission
459 size distributions. Secondly, the original emission size distributions in GAINS
460 contains from one to three different modes, whereas in AeroCom the
461 emissions are represented with only one mode. In many GAINS sources, e.g.
462 road transport, the mode with a larger mean emission diameter contributes
463 significantly to the emission of particles with $d_p > 100$ nm, even though the
464 total number emission is clearly dominated by a mode with a smaller mean
465 diameter. Finally, as stated earlier, the GAINS emission size distributions are
466 different for different technologies and fuels, in diesel powered road
467 transport also for different fuel sulfur contents. This increases the regional
468 variability of the emissions.

469

470 3.2 Simulated particle number concentrations and size distributions

471 Here we present the core of our analysis, which includes an assessment of
472 the modeled particle number concentrations against observations. Figure 4
473 shows the annual-averaged modeled particle concentration in comparison
474 with observations from eleven sites. Overall, both emission data sets showed
475 a tendency to underestimate particle number concentrations in model
476 simulations, especially for the locations with high observed particle number
477 concentrations. The underestimation of the highest particle concentrations
478 might be, at least partly, related to the spatial resolution of ECHAM-HAM, due
479 to which the typically high particle concentrations near urban or industrial
480 areas will be distributed evenly into a large model grid cell (Stier et al.,
481 2005). A comparison of the model results with the observational data shows
482 that the GAINS implementation significantly improved the reproduction of
483 observed concentrations in accumulation mode ($d_p > 100$ nm), being closer
484 to observations than AeroCom at all 11 sites. For the Aitken mode ($d_p = 10$ -
485 100 nm), similar improvement was not reached, as the observed
486 concentrations were better reproduced with AeroCom than with GAINS at 8
487 sites. The average relative bias described in Eq. (4) for the accumulation
488 mode concentrations with GAINS emissions was 2.37 and with AeroCom
489 emissions 3.51. The average relative bias for the Aitken mode concentrations

490 were 2.25 and 2.12 with GAINS and AeroCom emissions, respectively. It
491 should be noted that the emissions from different emission sources and
492 observations are not all from the same years. However, even though the
493 GAINS emissions are for year 2010 and AeroCom emissions for year 2000
494 (and observations for the years indicated in Table 2), the differences in the
495 modeled concentrations with GAINS and AeroCom at most polluted sites,
496 reaching factors of 2 and above, cannot be expected to originate from
497 differences in emissions between 2000 and 2010.

498 Figure 5 shows the modeled particle number size distributions against
499 observations at 6 measurement sites. The size distributions modeled with
500 the GAINS emissions agreed relatively well with the measurements for the
501 accumulation mode, whereas the nucleation and Aitken modes were
502 underestimated in simulations with both emission data sets. GAINS
503 underestimated the Aitken mode particle concentrations more heavily than
504 AeroCom, by a factor of two to three in Hyytiälä, Värriö and Kpuszta,
505 suggesting that the higher condensation sink associated with higher
506 accumulation mode particle emissions in GAINS had a significant impact on
507 modeled ultra-fine particle number concentrations. In addition, Hyytiälä and
508 Värriö are regions in which BVOC emissions and clean air are the key
509 influencing factors for new particle formation and particle growth (Ruuskanen
510 et al., 2007; Corrigan et al., 2013; Liao et al., 2014). This was reflected in the
511 model results: particle number size distributions in Hyytiälä and Värriö were
512 quite similar between the two simulations based on different anthropogenic
513 emission data sets. Contrary to this, Nanjing, Sao Paulo and Tomsok are areas
514 with strong influences by anthropogenic emissions, so that in comparison
515 with AeroCom, the simulations with GAINS emissions produced higher
516 accumulation mode and Aitken mode particle number concentrations as well
517 as better agreements with the observations in these regions. Nevertheless,
518 the model was not able to reach the observed ultra-fine particle
519 concentration in either simulation in most areas, and the higher CS in GAINS
520 significantly reduced particle number concentrations of the smallest particles
521 in most regions. Some areas showed a dramatic reduction in simulated ultra-
522 fine particle number concentrations e.g. in Nanjing the whole modeled
523 nucleation mode was wiped out when using the GAINS emissions.

524 The above results suggest that in ECHAM-HAM, as well as probably in other
525 climate models, the current nucleation and growth schemes may need
526 further revisions. However, it is also likely that the anthropogenic emissions

527 of especially nucleation mode particles in GAINS are still severely
528 underestimated for many source sectors (Paasonen et al., 2016). This is
529 because many of the measurements, on which the GAINS emission factors
530 are based, are not sensitive to non-solid nucleation mode particles, such as
531 those formed via nucleation of sulfur or organic vapors immediately after the
532 combustion or at small downwind distances in plumes from different
533 combustion sources (Stevens and Pierce, 2013). It should also be noted that
534 our study does not include any sensitivity analysis based on the primary
535 sulfate emissions parameterization (Luo and Yu, 2011). In addition, the lower
536 modeled Aitken mode particle concentrations from GAINS emissions may, in
537 some parts of the global domain, be also related to possible overestimations
538 in the accumulation mode particle emissions in the GAINS model, which are
539 consequently affecting the formation and growth of smaller particles.
540 Nonetheless, all the model versus observation comparisons between the
541 simulations clearly represent a consistent challenge for climate models in
542 modeling ultra-fine particle number size distributions.

543 Figure 6 shows absolute annual-average particle concentrations for the
544 accumulation mode and Aitken mode with both AeroCom and GAINS
545 emissions. While the regional distributions had similar patterns in both
546 simulations, there were evident differences when looking at the two size
547 modes. Accumulation mode particle concentrations were higher for the
548 simulation with the GAINS emission in most regions, which is consistent with
549 the input emissions assessment. The differences were particularly evident
550 over the developing areas where anthropogenic activities represent the main
551 source of atmospheric particles, especially in South America, central Africa,
552 India, China and south-east Asia. As observed in Figure 5, the high
553 accumulation mode particle number concentrations in the simulation with
554 the GAINS emission has a critical effect on Aitken mode particle
555 concentrations at most sites. A peculiar pattern is observed in China where
556 the dominant presence of anthropogenic sources from GAINS led the model
557 to predict high concentrations of ultra-fine particles. The decrease in GAINS-
558 derived Aitken mode particle number concentrations in areas where
559 emissions were actually higher than the AeroCom emission implies that
560 Aitken mode particles had been removed, or their secondary production was
561 hindered, by the prominent increase of the CS caused by a higher number of
562 emitted accumulation mode particles.

563

564 3.3 Concentrations and sources of CCN

565 This section presents the impact of particle emission data on atmospheric
566 CCN concentrations on annual and seasonal perspectives. It is important to
567 note that the applied anthropogenic number emissions did not have a
568 seasonal variation, so the seasonal differences are entirely due to the
569 variation of other emissions, and mainly to the strong temperature
570 dependence of biogenic SOA formation affecting the CCN concentration
571 (Paasonen et al., 2013). Our results showed clear differences in the simulated
572 CCN concentrations between the two primary emission data sets, and these
573 differences depended strongly on the considered supersaturation (Figure 7
574 and 8).

575 At the 0.2% supersaturation, the CCN concentrations were higher with the
576 GAINS emissions compared with the AeroCom emissions in practically all the
577 regions and during all seasons (Figure 8). The annual-average CCN_{0.2}
578 concentration ratio between the GAINS and AeroCom was two to three in
579 most areas, with peaks of four to ten in south America, central Africa and
580 east Asia (Figure 7). However, relatively high accumulation mode particle
581 concentrations were observed in India, China and south-east Asia (see Figure
582 6), and also an increase in absolute CCN_{0.2} concentration due to
583 anthropogenic emissions was observed in eastern China and south-east Asia.
584 Our analysis of the seasonality revealed that the difference between GAINS
585 and AeroCom simulations in terms of CCN_{0.2} concentrations was the largest
586 during the cold season in January, with boreal and arctic regions showing an
587 increment of GAINS/AeroCom CCN_{0.2} ratio up to a factor of seven to ten. The
588 southern hemisphere also displayed notable differences in both South
589 America and South-East Asia, with GAINS/AeroCom CCN_{0.2} ratios of three to
590 ten during the warmest season.

591 At the supersaturation of 1.0%, a significant fraction of Aitken mode particles
592 is capable of acting as CCN. Opposite to the CCN_{0.2} concentrations, the
593 simulated CCN_{1.0} concentrations with the GAINS emissions were lower than
594 with AeroCom emissions, with a GAINS/AeroCom ratio between 0.5 and 1 in
595 most regions (Figure 7). Our seasonality analysis showed that the simulation
596 with the GAINS data set produced higher CCN_{1.0} concentrations than
597 AeroCom in Europe, India and East Asia during the winter. However, such
598 ratio was equal to one or below in most regions, except eastern Asia, during
599 the warmer seasons. The substantially lower CCN_{1.0} concentrations with

600 GAINS emissions arise from the relatively similar Aitken mode number
601 emissions between GAINS and AeroCom, but significantly larger CS from
602 GAINS, causing a decrease in secondary ultrafine particle formation.
603 However, in China and South-East Asia, the annual CCN1.0 concentration
604 from GAINS was higher than from AeroCom by at least a factor of two,
605 suggesting that these regions may play a key role in contributing for the
606 global anthropogenic emissions and increment of CCN.

607 It is important to remark that the substantial differences in CCN
608 concentrations illustrated above are linked to the implementation of different
609 data sets, and therefore the modeled estimations might be affected by
610 uncertainties of the GAINS model as well. Furthermore, it may be questioned
611 whether the ECHAM-HAM is actually able to estimate CCN concentrations
612 with GAINS better than with AeroCom. This goes beyond the fundamental
613 goal of this study, which is to address the feasibility of using GAINS
614 emissions in global climate modeling. However, the modeled GAINS
615 accumulation mode particle number concentrations agree with observation
616 significantly better than AeroCom. This, based on the sensitivity analysis by
617 Lee et al. (2013), suggests that the GAINS implementation is likely to
618 estimate CCN concentrations better than AeroCom. In any case, further
619 studies are needed to address the contribution of the GAINS model in
620 improving modeled CCN concentration. Furthermore, it would be beneficial to
621 investigate how the applied nucleation scheme, combined with the GAINS
622 anthropogenic emissions, affects the estimation of CCN concentration to
623 better identify the driving forces behind the uncertainties of modeling
624 particle number size distributions with the global climate models.

625

626 4 Conclusions

627 The outcome of our experiment shows that the most significant differences
628 between the GAINS and AeroCom emissions data sets are (i) the particle size
629 distribution in the Aitken mode and accumulation mode, and (ii) the
630 geographical distribution of the particle number emissions over the global
631 domain. The accumulation mode particle emissions from GAINS are
632 significantly higher than AeroCom, by factors from 10 to 1000, thus
633 potentially resulting in dramatic increases in climatically active primary
634 particles and simultaneous decreases in secondary ultrafine particle
635 formation due to higher values of CS and coagulation sink.

636 In comparison to AeroCom emissions, GAINS emissions produced much
637 higher accumulation mode particle concentrations, but the consequently
638 higher CS and coagulation sink led to lower Aitken mode concentrations with
639 GAINS emissions than with AeroCom emissions. In comparison to observation
640 data at eleven measurement sites, the modeled annual-averaged
641 concentrations with GAINS emissions performed better than with AeroCom
642 emissions, in terms of bringing the modeled accumulation mode particle
643 concentrations closer to observation at all eleven sites, and Aitken mode
644 particle concentrations closer to observation at three sites. However, a
645 higher underestimation was observed in the simulation with GAINS emissions
646 for particles with $d_p < 30$ nm.

647 The underestimation of $d_p < 30$ nm particle concentrations in the simulation
648 with GAINS emissions highlighted the sensitivity of nucleation mode and
649 Aitken mode particle concentrations to CS and coagulation sink. This
650 underestimation is presumably partly caused by underestimations in
651 emissions of non-solid nucleation/Aitken mode particles in the GAINS model
652 (Paasonen et al., 2016). As a next step, the modules for nucleation and
653 subsequent growth and the sensitivity of the concentrations of sulfuric acid
654 (the main precursor in the applied nucleation parameterization) to altered CS
655 should be revisited.

656 It is important to note that the simulations performed in this study did not
657 implement an up-to-date secondary organic aerosols (ELVOCS) nucleation
658 scheme, nor a seasonal cycle of anthropogenic emissions, which may
659 represent a further step to reduce the gap between the modeled and
660 observed concentrations. Finally, given the high spatial variability of global
661 emissions, more observation data and the establishment of new
662 measurement stations in varying environments are urgently needed to better
663 evaluate the model results.

664

665 Acknowledgements

666 This project was funded by the MAJ JA TOR NESSLING grant n. 201600369
667 and the Academy of Finland Center of Excellence (FCoE) grant n. 307331.

668 Particle number size distributions at Melpitz were provided by Wolfram
669 Birmili, Kay Weinhold, André Sonntag, Birgit Wehner, Thomas Tuch, and

670 Alfred Wiedensohler (Leibniz Institute for Tropospheric Research, Leipzig,
671 Germany).

672 Particle number size distributions at Hohenpeissenberg were provided by
673 Harald Flentje and Björn Briel (German Weather Service, Hohenpeissenberg,
674 Germany). Both measurements were supported by the German Federal
675 Environment Ministry (BMU) grant UFOPLAN 370343200, project duration
676 2008-2010. Both data sets can be publicly accessed through the German
677 Ultrafine Aerosol Network (GUAN) at <https://doi.org/10.5072/guan>.

678 Particle number size distributions at Botsalano were provided by Ville Vakkari
679 and Lauri Laakso (Finnish Meteorological Institute, Helsinki, Finland).

680 Particle number size distributions at Sao Paulo were provided by John
681 Backman (Finnish Meteorological Institute, Helsinki, Finland).

682 Particle number size distributions at San Pietro Capofiume (Po Valley) were
683 provided by Ari Laaksonen (Finnish Meteorological Institute, Helsinki,
684 Finland).

685 We thank Chris Heyes and Zbigniew Klimont from the Air Quality and
686 Greenhouse Gases program at IIASA, and Kaarle Kupiainen from IIASA and
687 Finnish Environment Institute (SYKE) for their help and communication.

688 The EU FP7 BACCHUS project (grant n. 603445) and the Nordic Center of Excellence
689 eSTICC (Nordforsk grant n. 57001) are acknowledged for financial support.

690

691

692

693

694

695

696

697

698

- 700 Amann, M., Bertok, I., Borcken-Kleefeld, J., Cofala, J., Heyes, C., Höglund-Isaksson, L., Klimont,
701 Z., Nguyen, B., Posch, M., Rafaj, P., Sandler, R., Schöpp, W., Wagner, F. and Winiwarter, W.:
702 Cost-effective control of air quality and greenhouse gases in Europe: Modeling and policy
703 applications, *Environ. Model. Softw.*, 26(2), 1489–1501, 2011.
- 704
705 Backman, J., Rizzo, L. V., Hakala, J., Nieminen, T., Manninen, H. E., Morais, F., Aalto, P. P.,
706 Siivola, E., Carbone, S., Hillamo, R., Artaxo, P., Virkkula, A., Petäjä, T., and Kulmala, M.: On the
707 diurnal cycle of urban aerosols, black carbon and the occurrence of new particle formation
708 events in springtime São Paulo, Brazil, *Atmos. Chem. Phys.*, 12, 11733-11751,
709 doi:10.5194/acp-12-11733-2012, 2012.
- 710
711 Baker, L. H., Collins, W. J., Olivie, D. J. L., Cherian, R., Hodnebrog, Ø., Myhre, G., and Quaas,
712 J.: Climate responses to anthropogenic emissions of short-lived climate pollutants, *Atmos.*
713 *Chem. Phys.*, 15, 8201-8216, doi:10.5194/acp-15-8201-2015, 2015.
- 714
715 Berrisford, P., Kållberg, P., Kobayashi, S., Dee, D., Uppala, S., Simmons, A. J., Poli, P. and Sato,
716 H.: Atmospheric conservation properties in ERA-Interim. *Quarterly Journal of the Royal*
717 *Meteorological Society* 137:1381-1399, 2011.
- 718
719 Birmili, W., Weinhold, K., Rasch, F., Sonntag, A., Sun, J., Merkel, M., Wiedensohler, A., Bastian,
720 S., Schladitz, A., Löschau, G., Cyrus, J., Pitz, M., Gu, J., Kusch, T., Flentje, H., Quass, U.,
721 Kaminski, H., Kuhlbusch, T. A. J., Meinhardt, F., Schwerin, A., Bath, O., Ries, L., Gerwig, H.,
722 Wirtz, K., and Fiebig, M.: Long-term observations of tropospheric particle number size
723 distributions and equivalent black carbon mass concentrations in the German Ultrafine
724 Aerosol Network (GUAN), *Earth Syst. Sci. Data*, 8, 355-382, doi:10.5194/essd-8-355-2016,
725 2016.
- 726
727 Boucher, O., Randall, D., Artaxo, P., Bretherton, C., Feingold, G., Forster, P., Kerminen, V.-M.,
728 Kondo, Y., Liao, H., Lohmann, U., Rasch, P., Satheesh, S.K., Sherwood, S., Stevens, B. and
729 Zhang, X.Y.: Clouds and aerosols. In *Climate Change 2013: The Physical Science Basis.*
730 *Contribution of Working Group I to the Fifth Assessment Report of the Intergovernmental*
731 *Panel on Climate Change.* T.F. Stocker, D. Qin, G.-K. Plattner, M. Tignor, S.K. Allen, J.
732 Doschung, A. Nauels, Y. Xia, V. Bex, and P.M. Midgley, Eds. Cambridge University Press, 571-
733 657, doi:10.1017/CBO9781107415324.016, 2013.
- 734
735 Corrigan, A. L., Russell, L. M., Takahama, S., Äijälä, M., Ehn, M., Junninen, H., Rinne, J., Petäjä,
736 T., Kulmala, M., Vogel, A. L., Hoffmann, T., Ebben, C. J., Geiger, F. M., Chhabra, P., Seinfeld, J.
737 H., Worsnop, D. R., Song, W., Auld, J., and Williams, J.: Biogenic and biomass burning organic
738 aerosol in a boreal forest at Hyytiälä, Finland, during HUMPPA-COPEC 2010, *Atmos. Chem.*
739 *Phys.*, 13, 12233-12256, doi:10.5194/acp-13-12233-2013, 2013.
- 740
741 Dal Maso M., Sogacheva L., Anisimov M. P., Arshinov M., Baklanov A., Belan B., Khodzher T.
742 V., Obolkin V. A., Staroverova A., Vlasov A., Zagaynov V. A., Lushnikov A., Lyubovtseva Y. S.,
743 Riipinen I., Kerminen V.-M. and Kulmala M.: Aerosol particle formation events at two Siberian
744 stations inside the boreal forest. *Boreal Env. Res.* 13, 81-92, 2008.
- 745
746 Denier van der Gon, H., Visschedijk, A., Johansson, C., Hedberg Larsson, E., Harrison, R. M.,
747 and Beddows, D.: Size-resolved Pan European Anthropogenic Particle Number Inventory,
748 EUCAARI Deliverable 141, 2009.
- 749

750 Denier van der Gon, H., Visschedijk, A., Johansson, C., Ntziachristos, L., and Harrison, R. M.:
751 Size-resolved Pan-European Anthropogenic Particle Number Inventory, paper presented at
752 International Aerosol conference (oral), 29 August 3 September 2010, Helsinki, 2010.
753

754 Dentener, F., Kinne, S., Bond, T., Boucher, O., Cofala, J., Generoso, S., Ginoux, P., Gong, S.,
755 Hoelzemann, J. J., Ito, A., Marelli, L., Penner, J. E., Putaud, J.-P., Textor, C., Schulz, M., van der
756 Werf, G. R., and Wilson, J.: Emissions of primary aerosol and precursor gases in the years
757 2000 and 1750 prescribed data-sets for AeroCom, *Atmos. Chem. Phys.*, 6, 4321-4344,
758 doi:10.5194/acp-6-4321-2006, 2006.
759

760 Forster, P., Ramaswamy, V., Artaxo, P., Berntsen, T., Betts, R., Fahey, D.W., Haywood, J., Lean,
761 J., Lowe, D.C., Myhre, G., Nganga, J., Prinn, R., Raga, G., Schulz, M., Van Dorland, R. and
762 Miller, H.L.: *Changes in Atmospheric Constituents and in Radiative Forcing Chapter 2*. United
763 Kingdom: Cambridge University Press, 2007.
764

765 Guenther, A., Karl, T., Harley, P., Wiedinmyer, C., Palmer, P. I., and Geron, C.: Estimates of
766 global terrestrial isoprene emissions using MEGAN (Model of Emissions of Gases and
767 Aerosols from Nature), *Atmos. Chem. Phys.*, 6, 3181-3210, doi:10.5194/acp-6- 3181-2006,
768 2006.
769

770 Gultepe, I. Isaac, G.A.: Scale Effects on Averaging of Cloud Droplet and Aerosol Number
771 Concentrations: Observations and Models. *J. Climate* 12:1268-1279, 1999.
772

773 Hamed, A., Joutsensaari, J., Mikkonen, S., Sogacheva, L., Dal Maso, M., Kulmala, M., Cavalli,
774 F., Fuzzi, S., Facchini, M. C., Decesari, S., Mircea, M., Lehtinen, K. E. J., and Laaksonen, A.:
775 Nucleation and growth of new particles in Po Valley, Italy, *Atmos. Chem. Phys.*, 7, 355-376,
776 doi:10.5194/acp-7-355-2007, 2007.

777 Hari P., Kulmala M., Pohja T., Lahti T., Siivola E., Palva L., Aalto P., Hämeri K., Vesala T.,
778 Luoma S. and Pulliainen E.: Air pollution in Eastern Lapland: challenge for an
779 environmental measurement station. *Silva Fennica* 28: 29-39, 1994.

780 Hari, P. & Kulmala, M. Station for Measuring Ecosystem-Atmosphere Relations (SMEAR II).
781 *Boreal Env. Res.*, 10, 315-322, 2005.

782 Herrmann, E., Ding, A. J., Kerminen, V.-M., Petäjä, T., Yang, X. Q., Sun, J. N., Qi, X. M.,
783 Manninen, H., Hakala, J., Nieminen, T., Aalto, P. P., Kulmala, M., and Fu, C. B.: Aerosols and
784 nucleation in eastern China: first insights from the new SORPES-NJU station, *Atmos. Chem.*
785 *Phys.*, 14, 2169-2183, doi:10.5194/acp-14-2169-2014, 2014.
786

787 Hinds, W. C. (1982) *Aerosol Technology*, p. 85. Wiley, New York.
788

789 IPCC, *Climate Change: The Physical Science Basis. Contribution of Working Group I to the*
790 *Fifth Assessment Report of the Intergovernmental Panel on Climate Change* [Stocker, T.F., D.
791 Qin, G.-K. Plattner, M. Tignor, S.K. Allen, J. Boschung, A. Nauels, Y. Xia, V. Bex and P.M.
792 Midgley (eds.)]. Cambridge University Press, Cambridge, United Kingdom and New York, NY,
793 USA, 1535 pp, doi:10.1017/CBO9781107415324, 2013.
794

795 Jones, A., Haywood, J. M. and Boucher, O.: Aerosol forcing, climate response and climate
796 sensitivity in the Hadley Centre climate model, *J. Geophys. Res.*, 112, D20211,
797 doi:10.1029/2007JD008688, 2007.
798

799 Jokinen, T., Berndt, T., Makkonen, R., Kerminen, V., Junninen, H., Paasonen, P., Stratmann, F.,
800 Herrmann, H., Guenther, A.B., Worsnop, D.R., Kulmala, M., Ehn, M., Sipilä, M.: Production of
801 extremely low volatile organic compounds from biogenic emissions: Measured yields and
802 atmospheric implications, *Proceedings of the National Academy of Sciences* 112:7123-7128,
803 2015.
804
805 Kazil, J., Stier, P., Zhang, K., Quaas, J., Kinne, S., O'Donnell, D., Rast, S., Esch, M., Ferrachat,
806 S., Lohmann, U., and Feichter, J.: Aerosol nucleation and its role for clouds and Earth's
807 radiative forcing in the aerosol-climate model ECHAM5-HAM, *Atmos. Chem. Phys.*, 10,
808 10733-10752, doi:10.5194/acp-10-10733-2010, 2010.
809
810 Kerminen, V.-M., Kulmala, M.: Analytical formulae connecting the "real" and the "apparent"
811 nucleation rate and the nuclei number concentration for atmospheric nucleation events. *J*
812 *Aerosol Sci* 33(4):609-622, 2002.
813
814 Kerminen, V.-M., Paramonov, M., Anttila, T., Riipinen, I., Fountoukis, C., Korhonen, H., Asmi,
815 E., Laakso, L., Lihavainen, H., Swietlicki, E., Svenningsson, B., Asmi, A., Pandis, S. N.,
816 Kulmala, M., and Petäjä, T.: Cloud condensation nuclei production associated with
817 atmospheric nucleation: a synthesis based on existing literature and new results, *Atmos.*
818 *Chem. Phys.*, 12, 12037-12059, doi:10.5194/acp-12-12037-2012, 2012.
819
820 Kinne, S., Schulz, M., Textor, C., Guibert, S., Balkanski, Y., Bauer, S. E., Berntsen, T., Berglen,
821 T. F., Boucher, O., Chin, M., Collins, W., Dentener, F., Diehl, T., Easter, R., Feichter, J., Fillmore,
822 D., Ghan, S., Ginoux, P., Gong, S., Grini, A., Hendricks, J., Herzog, M., Horowitz, L., Isaksen, I.,
823 Iversen, T., Kirkevåg, A., Kloster, S., Koch, D., Kristjansson, J. E., Krol, M., Lauer, A.,
824 Lamarque, J. F., Lesins, G., Liu, X., Lohmann, U., Montanaro, V., Myhre, G., Penner, J., Pitari,
825 G., Reddy, S., Seland, O., Stier, P., Takemura, T., and Tie, X.: An AeroCom initial assessment –
826 optical properties in aerosol component modules of global models, *Atmos. Chem. Phys.*, 6,
827 1815-1834, doi:10.5194/acp-6-1815-2006, 2006.
828
829 Kiss, G., Varga, B., Galambos, I., & Ganszky, I. Characterization of water-soluble organic
830 matter isolated from atmospheric fine aerosol. *J. Geophys. Res.*, 107, 8339-8347,
831 doi:10.1029/2001JD000603, 2002.
832
833 Klimont, Z., Kupiainen, K., Heyes, C., Purohit, P., Cofala, J., Rafaj, P., Borcken-Kleefeld, J. and
834 Schöpp, W.: Global anthropogenic emissions of particulate matter including black carbon,
835 *Atmospheric Chem. Phys. Discuss.*, 2016, 1-72, doi:10.5194/acp-2016-880, 2016.
836
837 Kloster, S., Feichter, J., Maier-Reimer, E., Six, K. D., Stier, P., and Wetzzel, P.: DMS cycle in the
838 marine ocean-atmosphere system – a global model study, *Biogeosciences*, 3, 29-51,
839 doi:10.5194/bg-3-29-2006, 2006.
840
841 Kooperman, G. J., Pritchard, M. S., Ghan, S. J., Wang, M., Somerville, R. C. J., and Russell, L.
842 M.: Constraining the influence of natural variability to improve estimates of global aerosol
843 indirect effects in a nudged version of the Community Atmosphere Model 5, *J. Geophys. Res.*,
844 117, D23204, doi:10.1029/2012JD018588, 2012.
845
846 Kulmala, M., Dal Maso, M., Mäkelä, J., Pirjola, L., Väkevä, M., Aalto, P., Miikkulainen, P.,
847 Hämeri, K., and O'dowd, C.: On the formation, growth and composition of nucleation mode
848 particles. *Tellus B*, 53(4). doi:http://dx.doi.org/10.3402/tellusb.v53i4.16622, 2001.
849

850 Kupiainen, K. and Klimont, Z.: Primary emissions of fine carbonaceous particles in Europe.
851 Atmospheric Environment 41:2156 – 2170, 2007.
852

853 Laakso, L., Laakso, H., Aalto, P. P., Keronen, P., Petäjä, T., Nieminen, T., Pohja, T., Siivola, E.,
854 Kulmala, M., Kgabi, N., Molefe, M., Mabaso, D., Phalatse, D., Pienaar, K., and Kerminen, V.-M.:
855 Basic characteristics of atmospheric particles, trace gases and meteorology in a relatively
856 clean Southern African Savannah environment, Atmos. Chem. Phys., 8, 4823-4839,
857 doi:10.5194/acp-8-4823-2008, 2008.
858

859 Lee, L. A., Pringle, K. J., Reddington, C. L., Mann, G. W., Stier, P., Spracklen, D. V., Pierce, J. R.,
860 and Carslaw, K. S.: The magnitude and causes of uncertainty in global model simulations of
861 cloud condensation nuclei, Atmos. Chem. Phys., 13, 8879-8914, doi:10.5194/acp-13-8879-
862 2013, 2013.
863

864 Liao, L., Kerminen, V.-M., Boy, M., Kulmala, M., and Dal Maso, M.: Temperature influence on
865 the natural aerosol budget over boreal forests, Atmos. Chem. Phys., 14, 8295-8308,
866 doi:10.5194/acp-14-8295-2014, 2014.
867

868 Lohmann, U. and Feichter, J.: Global indirect aerosol effects: a review, Atmos. Chem. Phys.,
869 5, 715-737, doi:10.5194/acp-5-715-2005, 2005.
870

871 Luo, G. and Yu, F.: Sensitivity of global cloud condensation nuclei concentrations to primary
872 sulfate emission parameterizations, Atmos. Chem. Phys., 11, 1949-1959,
873 <https://doi.org/10.5194/acp-11-1949-2011>, 2011.
874

875 Makkonen, R., Asmi, A., Korhonen, H., Kokkola, H., Järvenoja, S., Räisänen, P., Lehtinen, K. E.
876 J., Laaksonen, A., Kerminen, V.-M., Järvinen, H., Lohmann, U., Bennartz, R., Feichter, J., and
877 Kulmala, M.: Sensitivity of aerosol concentrations and cloud properties to nucleation and
878 secondary organic distribution in ECHAM5-HAM global circulation model, Atmos. Chem.
879 Phys., 9, 1747-1766, doi:10.5194/acp-9-1747-2009, 2009.
880

881 Makkonen, R., Asmi, A., Kerminen, V.-M., Boy, M., Arneth, A., Guenther, A., and Kulmala, M.:
882 BVOC-aerosol-climate interactions in the global aerosol-climate model ECHAM5.5-HAM2,
883 Atmos. Chem. Phys., 12, 10077-10096, doi:10.5194/acp-12-10077-2012, 2012.
884

885 Makkonen, R., Seland, Ø., Kirkevåg, A., Iversen, T., and Kristjánsson, J. E.: Evaluation of
886 aerosol number concentrations in NorESM with improved nucleation parameterization,
887 Atmos. Chem. Phys., 14, 5127-5152, doi:10.5194/acp-14-5127-2014, 2014.
888

889 Merikanto, J., Spracklen, D. V., Mann, G. W., Pickering, S. J., and Carslaw, K. S.: Impact of
890 nucleation on global CCN, Atmos. Chem. Phys., 9, 8601-8616, doi:10.5194/acp-9-8601-2009,
891 2009.
892

893 Paasonen, P., Asmi, A., Petaja, T., Kajos, M.K, Aijala, M, Junninen, H, Holst, T, Abbatt, J.P.D,
894 Arneth, A, Birmili, W, van der Gon, H.D, Hamed, A, Hoffer, A, Laakso, L, Laaksonen, A,
895 Richard Leaitch, W, Plass-Dulmer, C, Pryor, S.C, Raisanen, P, Swietlicki, E, Wiedensohler, A,
896 Worsnop, D.R, Kerminen, V, Kulmala, M.: Warming-induced increase in aerosol number
897 concentration likely to moderate climate change. Nature Geoscience 6:438-442, 2013.
898

899 Paasonen, P., Kupiainen, K., Klimont, Z., Visschedijk, A., Denier van der Gon, H. A. C., and
900 Amann, M.: Continental anthropogenic primary particle number emissions, Atmos. Chem.
901 Phys., 16, 6823-6840, doi:10.5194/acp-16-6823-2016, 2016.
902

903 Pozzoli, L., Janssens-Maenhout, G., Diehl, T., Bey, I., Schultz, M. G., Feichter, J., Vignati, E.,
904 and Dentener, F.: Re-analysis of tropospheric sulfate aerosol and ozone for the period 1980-
905 2005 using the aerosol-chemistry-climate model ECHAM5-HAMMOZ, *Atmos. Chem. Phys.*, 11,
906 9563-9594, doi:10.5194/acp-11-9563-2011, 2011.

907

908 Riipinen, I., Pierce, J. R., Yli-Juuti, T., Nieminen, T., Häkkinen, S., Ehn, M., Junninen, H.,
909 Lehtipalo, K., Petäjä, T., Slowik, J., Chang, R., Shantz, N. C., Abbatt, J., Leaitch, W. R.,
910 Kerminen, V.-M., Worsnop, D. R., Pandis, S. N., Donahue, N. M., and Kulmala, M.: Organic
911 condensation: a vital link connecting aerosol formation to cloud condensation nuclei (CCN)
912 concentrations, *Atmos. Chem. Phys.*, 11, 3865-3878, doi:10.5194/acp-11-3865-2011, 2011.

913

914 Roelofs, G.-J., ten Brink, H., Kiendler-Scharr, A., de Leeuw, G., Mensah, A., Minikin, A., and
915 Otjes, R.: Evaluation of simulated aerosol properties with the aerosol-climate model
916 ECHAM5-HAM using observations from the IMPACT field campaign, *Atmos. Chem. Phys.*, 10,
917 7709-7722, doi:10.5194/acp-10-7709-2010, 2010.

918

919 Ruuskanen, T. M., Kaasik, M., Aalto, P. P., Hörrak, U., Vana, M., Mårtensson, M., Yoon, Y. J.,
920 Keronen, P., Mordas, G., Ceburnis, D., Nilsson, E. D., O'Dowd, C., Noppel, M., Alliksaar, T.,
921 Ivask, J., Sofiev, M., Prank, M., and Kulmala, M.: Concentrations and fluxes of aerosol
922 particles during the LAPBIAT measurement campaign at Värriö field station, *Atmos. Chem.*
923 *Phys.*, 7, 3683-3700, doi:10.5194/acp-7-3683-2007, 2007.

924

925 Samset, B. H., Myhre, G., Herber, A., Kondo, Y., Li, S.-M., Moteki, N., Koike, M., Oshima, N.,
926 Schwarz, J. P., Balkanski, Y., Bauer, S. E., Bellouin, N., Berntsen, T. K., Bian, H., Chin, M., Diehl,
927 T., Easter, R. C., Ghan, S. J., Iversen, T., Kirkevåg, A., Lamarque, J.-F., Lin, G., Liu, X., Penner, J.
928 E., Schulz, M., Seland, Ø., Skeie, R. B., Stier, P., Takemura, T., Tsigaridis, K., and Zhang, K.:
929 Modelled black carbon radiative forcing and atmospheric lifetime in AeroCom Phase II
930 constrained by aircraft observations, *Atmos. Chem. Phys.*, 14, 12465-12477,
931 doi:10.5194/acp-14-12465-2014, 2014.

932

933 Schulz, M., Textor, C., Kinne, S., Balkanski, Y., Bauer, S., Berntsen, T., Berglen, T., Boucher, O.,
934 Dentener, F., Guibert, S., Isaksen, I. S. A., Iversen, T., Koch, D., Kirkevåg, A., Liu, X.,
935 Montanaro, V., Myhre, G., Penner, J. E., Pitari, G., Reddy, S., Seland, Ø., Stier, P., and
936 Takemura, T.: Radiative forcing by aerosols as derived from the AeroCom present-day and
937 pre-industrial simulations, *Atmos. Chem. Phys.*, 6, 5225-5246, doi:10.5194/acp-6-5225-2006,
938 2006.

939

940 Schurgers, G., Arneth, A., Holzinger, R., and Goldstein, A. H.: Process-based modelling of
941 biogenic monoterpene emissions combining production and release from storage, *Atmos.*
942 *Chem. Phys.*, 9, 3409-3423, doi:10.5194/acp-9-3409-2009, 2009.

943

944 Schutgens, N. A. J., Gryspeerdt, E., Weigum, N., Tsyro, S., Goto, D., Schulz, M., and Stier, P.:
945 Will a perfect model agree with perfect observations? The impact of spatial sampling, *Atmos.*
946 *Chem. Phys.*, 16, 6335-6353, doi:10.5194/acp-16-6335-2016, 2016.

947

948 Seinfeld, J. H. and Pandis, S. N.: *Atmospheric Chemistry and Physics: From Air Pollution to*
949 *Climate Change*, John Wiley and Sons, 1998.

950

951 Shilling, J. E., Zaveri, R. A., Fast, J. D., Kleinman, L., Alexander, M. L., Canagaratna, M. R.,
952 Fortner, E., Hubbe, J. M., Jayne, J. T., Sedlacek, A., Setyan, A., Springston, S., Worsnop, D. R.,
953 and Zhang, Q.: Enhanced SOA formation from mixed anthropogenic and biogenic emissions
954 during the CARES campaign, *Atmos. Chem. Phys.*, 13, 2091-2113, doi:10.5194/acp-13-2091-
955 2013, 2013.

956
957 Shindell, D. T., Faluvegi, G., Bauer, S. E., Koch, D. M., Unger, N., Menon, S., Miller, R. L.,
958 Schmidt, G. A. and Streets, D. G.: Climate response to projected changes in short-lived
959 species under an A1B scenario from 2000–2050 in the GISS climate model, *J. Geophys. Res.*,
960 112, D20103, doi:10.1029/2007JD008753, 2007.

961
962 Spracklen, D. V., Carslaw, K. S., Kulmala, M., Kerminen, V.-M., Mann, G. W., and Sihto, S.-L.:
963 The contribution of boundary layer nucleation events to total particle concentrations on
964 regional and global scales, *Atmos. Chem. Phys.*, 6, 5631-5648, doi:10.5194/acp-6-5631-
965 2006, 2006.

966
967 Spracklen, D. V., Carslaw, K. S., Kerminen, V.-M., Sihto, S.-L., Riipinen, I., Merikanto, J., Mann,
968 G. W., Chipperfield, M. P., Wiedensohler, A., Birmili, W. and Lihavainen, H.: Contribution of
969 particle formation to global cloud condensation nuclei concentrations, *Geophys. Res. Lett.*,
970 35, L06808, doi:10.1029/2007GL033038.

971
972 Spracklen, D. V., Carslaw, K. S., Merikanto, J., Mann, G. W., Reddington, C. L., Pickering, S.,
973 Ogren, J. A., Andrews, E., Baltensperger, U., Weingartner, E., Boy, M., Kulmala, M., Laakso, L.,
974 Lihavainen, H., Kivekäs, N., Komppula, M., Mihalopoulos, N., Kouvarakis, G., Jennings, S. G.,
975 O'Dowd, C., Birmili, W., Wiedensohler, A., Weller, R., Gras, J., Laj, P., Sellegri, K., Bonn, B.,
976 Krejci, R., Laaksonen, A., Hamed, A., Minikin, A., Harrison, R. M., Talbot, R., and Sun, J.:
977 Explaining global surface aerosol number concentrations in terms of primary emissions and
978 particle formation, *Atmos. Chem. Phys.*, 10, 4775-4793, doi:10.5194/acp-10-4775-2010,
979 2010.

980
981 Spracklen, D. V., Jimenez, J. L., Carslaw, K. S., Worsnop, D. R., Evans, M. J., Mann, G. W.,
982 Zhang, Q., Canagaratna, M. R., Allan, J., Coe, H., McFiggans, G., Rap, A., and Forster, P.:
983 Aerosol mass spectrometer constraint on the global secondary organic aerosol budget,
984 *Atmos. Chem. Phys.*, 11, 12109-12136, doi:10.5194/acp-11-12109-2011, 2011.

985
986 Stevens, R. G. and Pierce, J. R.: A parameterization of sub-grid particle formation in sulfur-
987 rich plumes for global- and regional-scale models, *Atmos. Chem. Phys.*, 13, 12117-12133,
988 doi:10.5194/acp-13-12117-2013, 2013.

989
990 Stier, P., Feichter, J., Kinne, S., Kloster, S., Vignati, E., Wilson, J., Ganzeveld, L., Tegen, I.,
991 Werner, M., Balkanski, Y., Schulz, M., Boucher, O., Minikin, A., and Petzold, A.: The aerosol-
992 climate model ECHAM5-HAM, *Atmos. Chem. Phys.*, 5, 1125-1156, doi:10.5194/acp-5-1125-
993 2005, 2005.

994
995 Stier, P., Seinfeld, J. H., Kinne, S., and Boucher, O.: Aerosol absorption and radiative forcing,
996 *Atmos. Chem. Phys.*, 7, 5237-5261, doi:10.5194/acp-7-5237-2007, 2007.

997
998 Stohl, A., Aamaas, B., Amann, M., Baker, L. H., Bellouin, N., Berntsen, T. K., Boucher, O.,
999 Cherian, R., Collins, W., Daskalakis, N., Dusinska, M., Eckhardt, S., Fuglestad, J. S., Harju,
1000 M., Heyes, C., Hodnebrog, Ø., Hao, J., Im, U., Kanakidou, M., Klimont, Z., Kupiainen, K., Law,
1001 K. S., Lund, M. T., Maas, R., MacIntosh, C. R., Myhre, G., Myriokefalitakis, S., Olivé, D., Quaas,
1002 J., Quennehen, B., Raut, J.-C., Rumbold, S. T., Samset, B. H., Schulz, M., Seland, Ø., Shine, K.
1003 P., Skeie, R. B., Wang, S., Yttri, K. E., and Zhu, T.: Evaluating the climate and air quality
1004 impacts of short-lived pollutants, *Atmos. Chem. Phys.*, 15, 10529-10566, doi:10.5194/acp-
1005 15-10529-2015, 2015.

1006
1007 Textor, C., Schulz, M., Guibert, S., Kinne, S., Balkanski, Y., Bauer, S., Berntsen, T., Berglen, T.,
1008 Boucher, O., Chin, M., Dentener, F., Diehl, T., Easter, R., Feichter, H., Fillmore, D., Ghan, S.,

1009 Ginoux, P., Gong, S., Grini, A., Hendricks, J., Horowitz, L., Huang, P., Isaksen, I., Iversen, I.,
 1010 Kloster, S., Koch, D., Kirkevåg, A., Kristjansson, J. E., Krol, M., Lauer, A., Lamarque, J. F., Liu,
 1011 X., Montanaro, V., Myhre, G., Penner, J., Pitari, G., Reddy, S., Seland, Ø., Stier, P., Takemura,
 1012 T., and Tie, X.: Analysis and quantification of the diversities of aerosol life cycles within
 1013 AeroCom, *Atmos. Chem. Phys.*, 6, 1777-1813, doi:10.5194/acp-6-1777-2006, 2006.
 1014
 1015 Tonttila, J., Järvinen, H., and Räisänen, P.: Explicit representation of subgrid variability in
 1016 cloud microphysics yields weaker aerosol indirect effect in the ECHAM5-HAM2 climate model,
 1017 *Atmos. Chem. Phys.*, 15, 703-714, doi:10.5194/acp-15-703-2015, 2015.
 1018
 1019 Tsigaridis, K., Daskalakis, N., Kanakidou, M., Adams, P. J., Artaxo, P., Bahadur, R., Balkanski,
 1020 Y., Bauer, S. E., Bellouin, N., Benedetti, A., Bergman, T., Berntsen, T. K., Beukes, J. P., Bian, H.,
 1021 Carslaw, K. S., Chin, M., Curci, G., Diehl, T., Easter, R. C., Ghan, S. J., Gong, S. L., Hodzic, A.,
 1022 Hoyle, C. R., Iversen, T., Jathar, S., Jimenez, J. L., Kaiser, J. W., Kirkevåg, A., Koch, D., Kokkola,
 1023 H., Lee, Y. H., Lin, G., Liu, X., Luo, G., Ma, X., Mann, G. W., Mihalopoulos, N., Morcrette, J.-J.,
 1024 Müller, J.-F., Myhre, G., Myriokefalitakis, S., Ng, N. L., O'Donnell, D., Penner, J. E., Pozzoli, L.,
 1025 Pringle, K. J., Russell, L. M., Schulz, M., Sciare, J., Seland, Ø., Shindell, D. T., Sillman, S., Skeie,
 1026 R. B., Spracklen, D., Stavroukou, T., Steenrod, S. D., Takemura, T., Tiitta, P., Tilmes, S., Tost, H.,
 1027 van Noije, T., van Zyl, P. G., von Salzen, K., Yu, F., Wang, Z., Wang, Z., Zaveri, R. A., Zhang,
 1028 H., Zhang, K., Zhang, Q., and Zhang, X.: The AeroCom evaluation and intercomparison of
 1029 organic aerosol in global models, *Atmos. Chem. Phys.*, 14, 10845-10895, doi:10.5194/acp-
 1030 14-10845-2014, 2014.
 1031
 1032 Turpin, B.J., Saxena, P., Andrews, E.: Measuring and simulating particulate organics in the
 1033 atmosphere: problems and prospects. *Atmospheric Environment* 34:2983-3013, 2000.
 1034
 1035 van Ulden, A. and Wieringa, J.: Atmospheric boundary layer re- search at Cabauw, *Bound.-*
 1036 *Lay. Meteorol.*, 78, 39-69, 1996.
 1037
 1038 Vignati, E., Wilson, J. and Stier, P.: M7: An efficient size-resolved aerosol microphysics module
 1039 for large-scale aerosol transport models, *J. Geophys. Res.*, 109, D22202,
 1040 doi:10.1029/2003JD004485, 2004.
 1041
 1042 Zhang, K., O'Donnell, D., Kazil, J., Stier, P., Kinne, S., Lohmann, U., Ferrachat, S., Croft, B.,
 1043 Quaas, J., Wan, H., Rast, S., and Feichter, J.: The global aerosol-climate model ECHAM-HAM,
 1044 version 2: sensitivity to improvements in process representations, *Atmos. Chem. Phys.*, 12,
 1045 8911-8949, doi:10.5194/acp-12-8911-2012, 2012.
 1046
 1047 Zhang, S., Wang, M., Ghan, S. J., Ding, A., Wang, H., Zhang, K., Neubauer, D., Lohmann, U.,
 1048 Ferrachat, S., Takeamura, T., Gettelman, A., Morrison, H., Lee, Y., Shindell, D. T., Partridge, D.
 1049 G., Stier, P., Kipling, Z., and Fu, C.: On the characteristics of aerosol indirect effect based on
 1050 dynamic regimes in global climate models, *Atmos. Chem. Phys.*, 16, 2765-2783,
 1051 doi:10.5194/acp-16-2765-2016, 2016.
 1052
 1053
 1054
 1055
 1056
 1057
 1058
 1059

TABLES

1060
1061
1062
1063
1064
1065
1066

Table 1. Input data provided from AeroCom inventory and GAINS model for submicron particle emissions. The data is sorted according to its original structure in terms of mass, number, chemical species differentiation (BC, OC and SO₄), bi-level vertical distribution (2-zL) and base year. (✓) and (✗) indicate whether the data set contains a certain information or not, respectively.

Data	M	N	Species	2-zL	Year
AeroCom	✓	✗	✓	✓	2000
GAINS	✗	✓	✗	✗	2010

1067
1068
1069
1070
1071
1072
1073
1074
1075
1076
1077
1078
1079
1080
1081
1082
1083
1084

1085 Table 2. Description of measurement sites for model versus observation evaluation.

Station	Lon	Lat	m. a. s. l.	Years	Reference
Botsalano, South Africa	25.8 ° E	25.5 ° S	1424	07/2006-08/2007	Laakso et al., 2008.
Cabauw, Netherlands	4.9 ° E	52.0 ° N	60	04/2008-03/2009	van Ulden and Wieringa, 1996.
Hohenpeissenberg, Germany	11.0 ° E	47.8 ° N	980	06/2007-11/2008	Birmili et al., 2016.
Hyytiälä, Finland	24.3 ° E	61.9 ° N	180	01/2009-12/2010	Hari and Kulmala, 2005.
K-Pusztá, Hungary	19.6 ° E	47.0 ° N	125	03/2007-03/2009	Kiss et al., 2002.
Melpitz, Germany	12.9 ° E	51.5 ° N	84	01/2007-12/2008	Birmili et al., 2016.
Nanjing, China	118.9 ° E	32.1 ° N	40	12/2011-12/2014	Herrmann et al., 2014.
Po Valley, Italy	11.6 ° E	44.7 ° N	11	09/2004-09/2006	Hamed et al., 2007.
Sao Paulo, Brazil	46.7 ° W	23.5 ° S	760	10/2010-09/2011	Backman et al., 2012.
Tomsk FNV, Russia	84.1 ° E	56.4 ° N	80	01/2012-12/2013	Dal Maso et al., 2008.
Värriö, Finland	29.6 ° E	67.8 ° N	400	01/2009-12/2011	Hari et al., 1994.

1086

1087 Table 3. Annual total particle number (second and third columns) and global average ratios
 1088 (fourth and fifth columns) of input emissions computed for the whole domain. R_{tot} ratios are
 1089 calculated by firstly averaging the emissions among the whole domain for each data set,
 1090 and secondly divide GAINS by AeroCom. This method aims at studying absolute differences
 1091 in the global emissions with no regard to geographical distribution differences. In R_{grid} we
 1092 firstly divide the data sets to keep the information of data sets differences for each grid cell,
 1093 and secondly compute the median of gridded ratios. R_{grid} is weighted by surface area of the
 1094 grid cell.

Global emissions	AeroCom 10^{25} yr^{-1}	GAINS 10^{25} yr^{-1}	R_{tot} mean	R_{grid} median
Total	3.42	7.39	2.16	1.00
Accumulation	0.028	1.74	62.14	48.65
Aitken	3.39	5.66	1.67	0.71

1095

1096

1097 Table 4. Modeled global annually-averaged concentrations of total particle, CCN0.2 and
 1098 CCN1,0 with AeroCom and GAINS data sets (second and third columns). Continental and
 1099 (global) average ratios of total particle and CCN concentrations were calculated as in Table
 1100 3.

Global concentrations	AeroCom 10^{12} m^{-3}	GAINS 10^{12} m^{-3}	R_{tot} mean	R_{grid} median
Total	37.08	33.98	0.83 (0.91)	0.96 (0.99)
CCN0.2	1.65	2.47	1.69 (1.49)	1.16 (1.04)
CCN1.0	7.04	6.77	0.96 (0.96)	0.99 (0.98)

1101

1102

1103

1104

1105

1106

1107

1108

1109

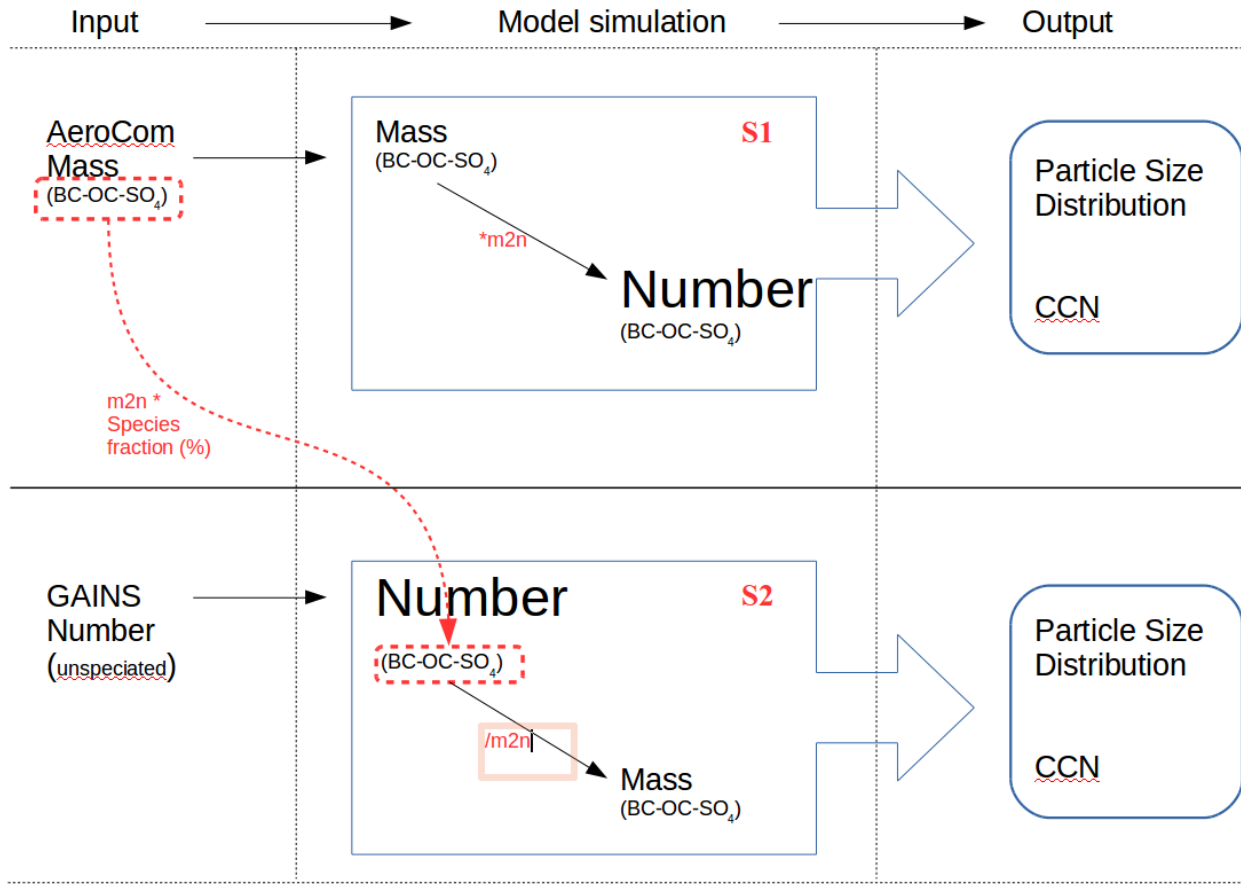
1110

1111

1112

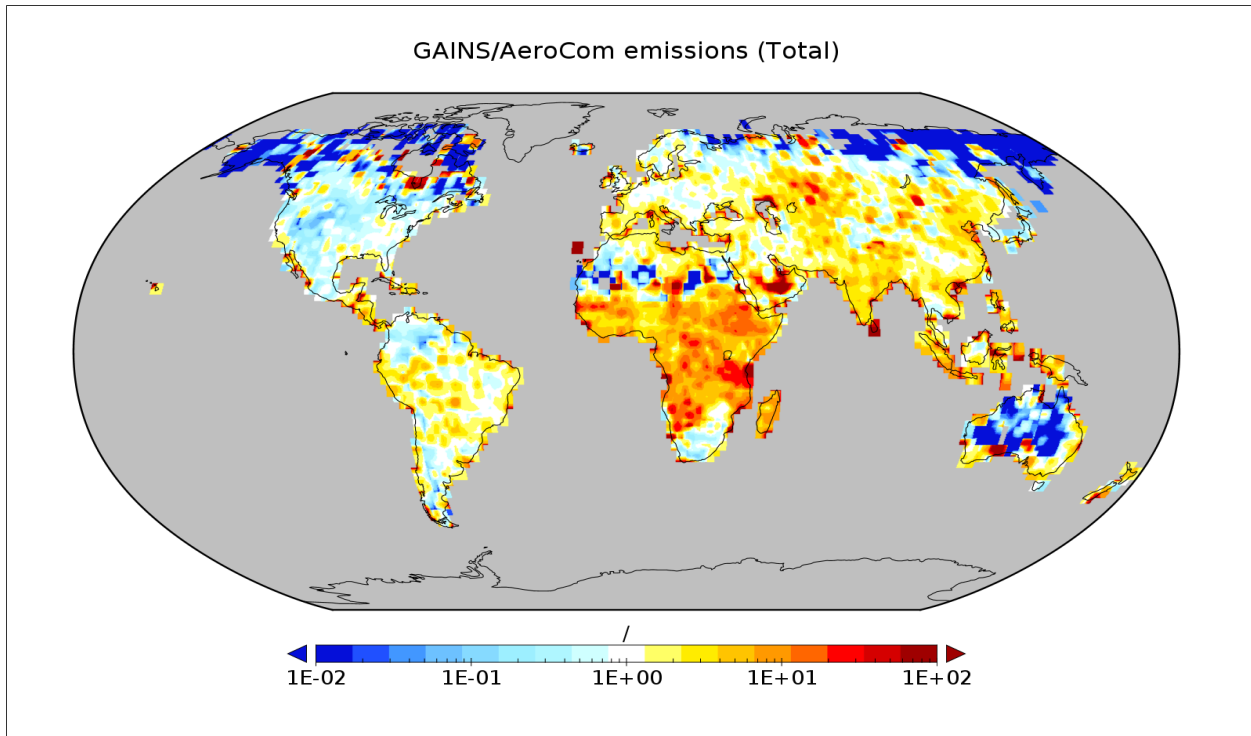
1113
1114

FIGURES



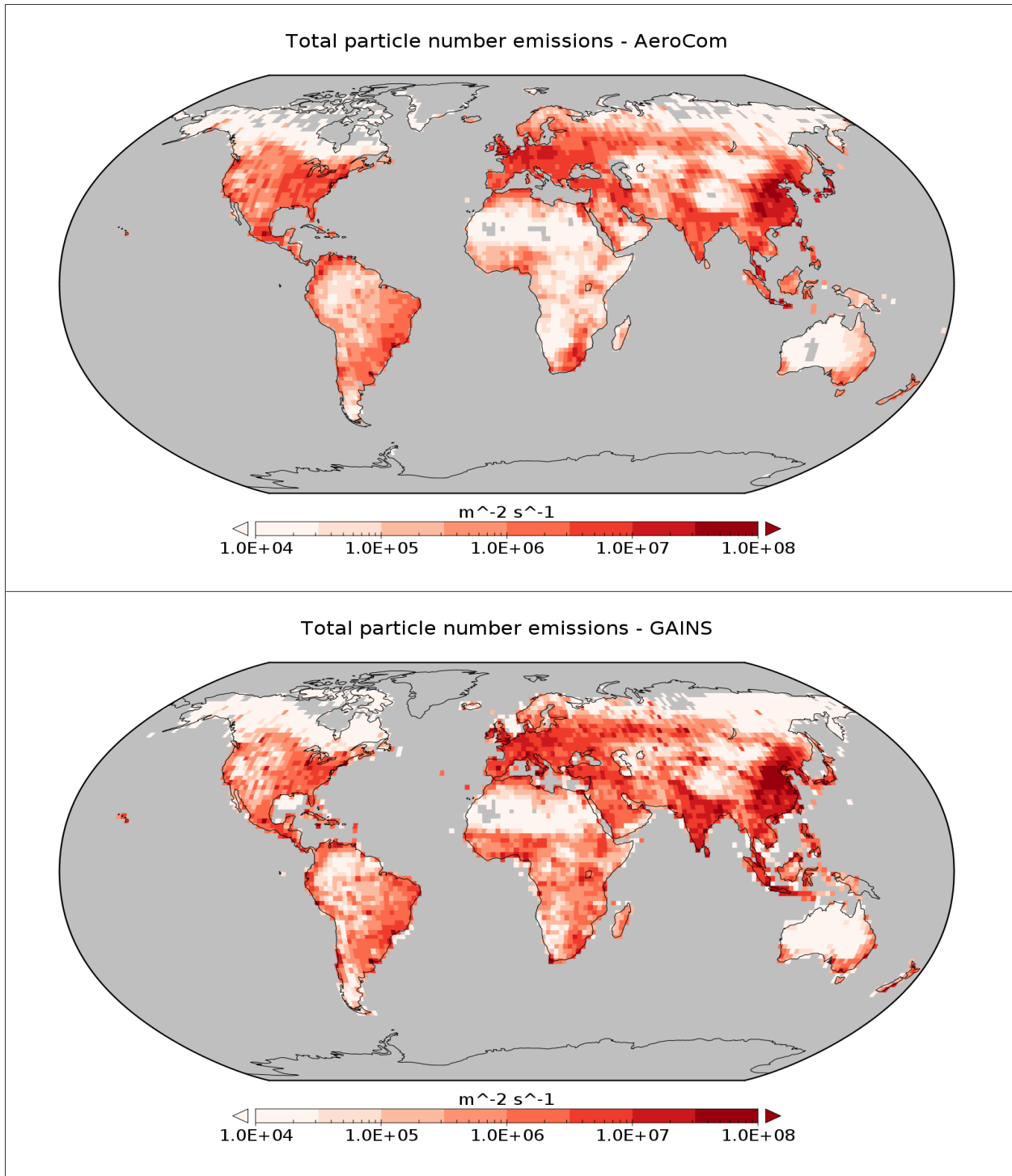
1116 Figure 1. Framework describing the off-line steps to implement GAINS mass and number
1117 anthropogenic emissions in the ECHAM-HAM. The AeroCom mass-to-number (m_{2n})
1118 conversion factors and the chemical species fractions (%) of AeroCom number emissions
1119 were used to speciate GAINS number emissions. A specific m_{2n} factor was used for each
1120 species for either mass-to-number ($*m_{2n}$) or number-to-mass ($/m_{2n}$) conversion.

1121
1122
1123
1124
1125
1126
1127
1128

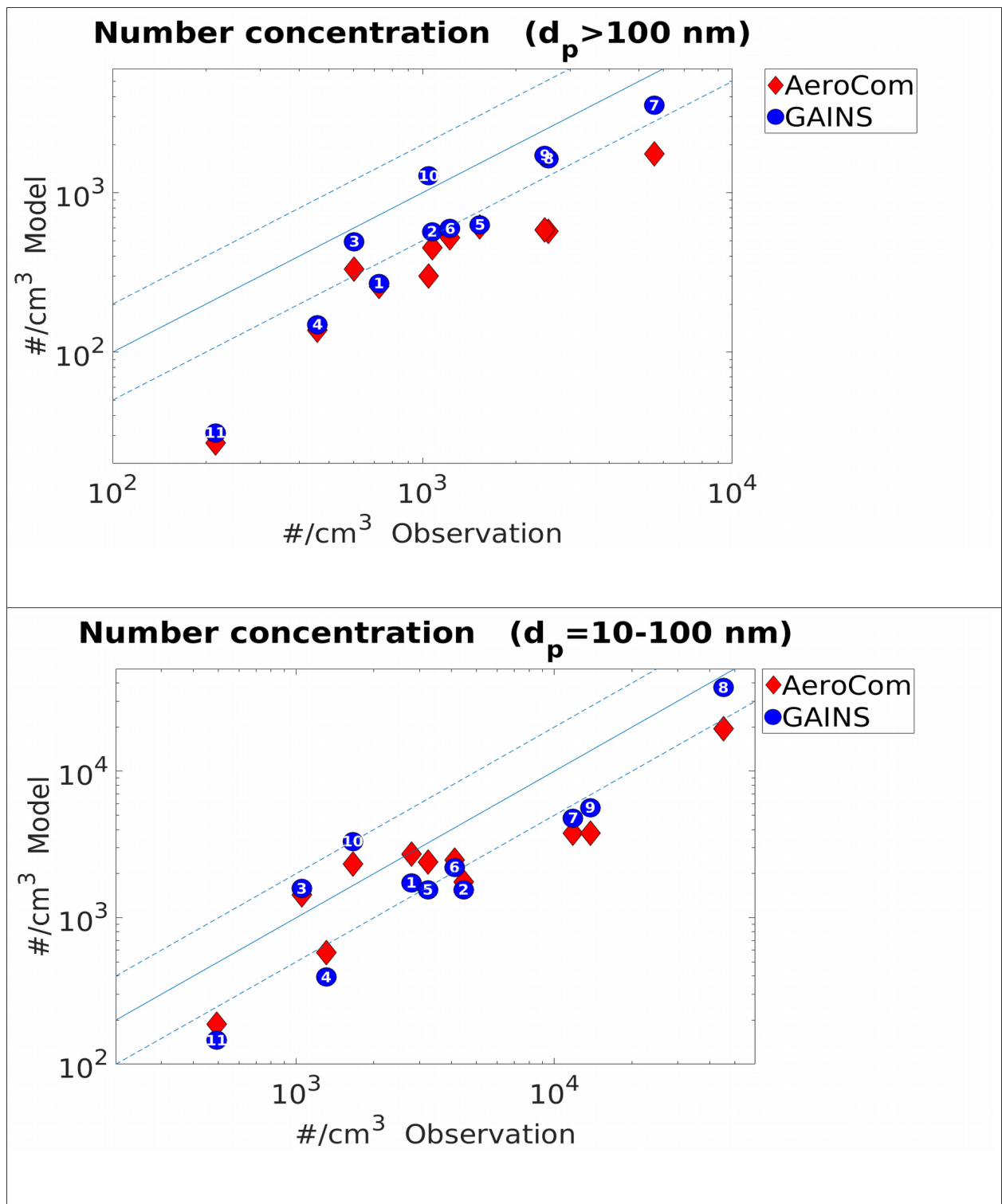


1129 Figure 2. GAINS/AeroCom ratio for annual particle number emissions.

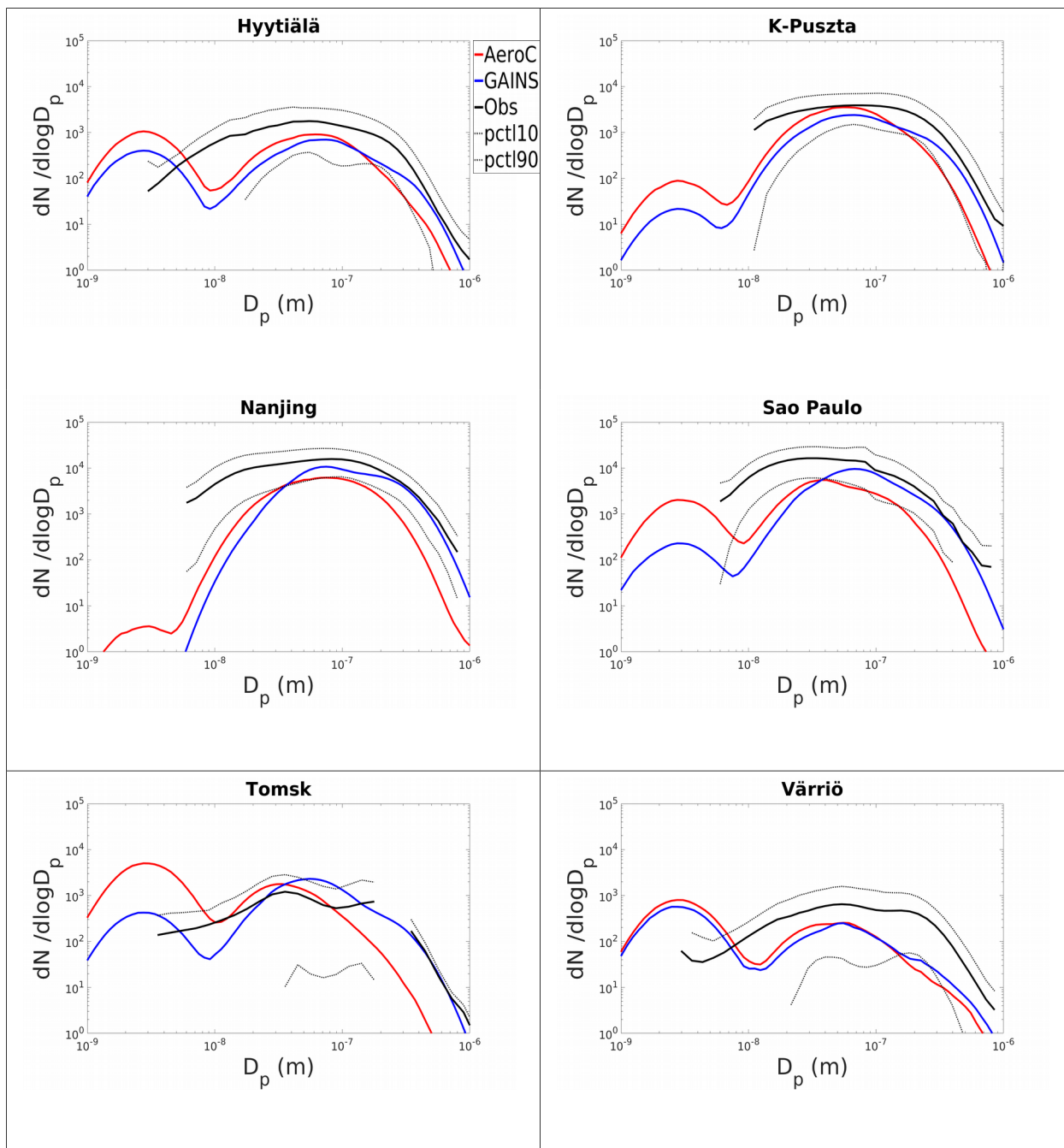
1130
1131
1132
1133
1134
1135
1136
1137
1138
1139
1140
1141
1142



1143 Figure 3. Total absolute emissions for (a) AeroCom and (b) GAINS without visual
1144 interpolation.

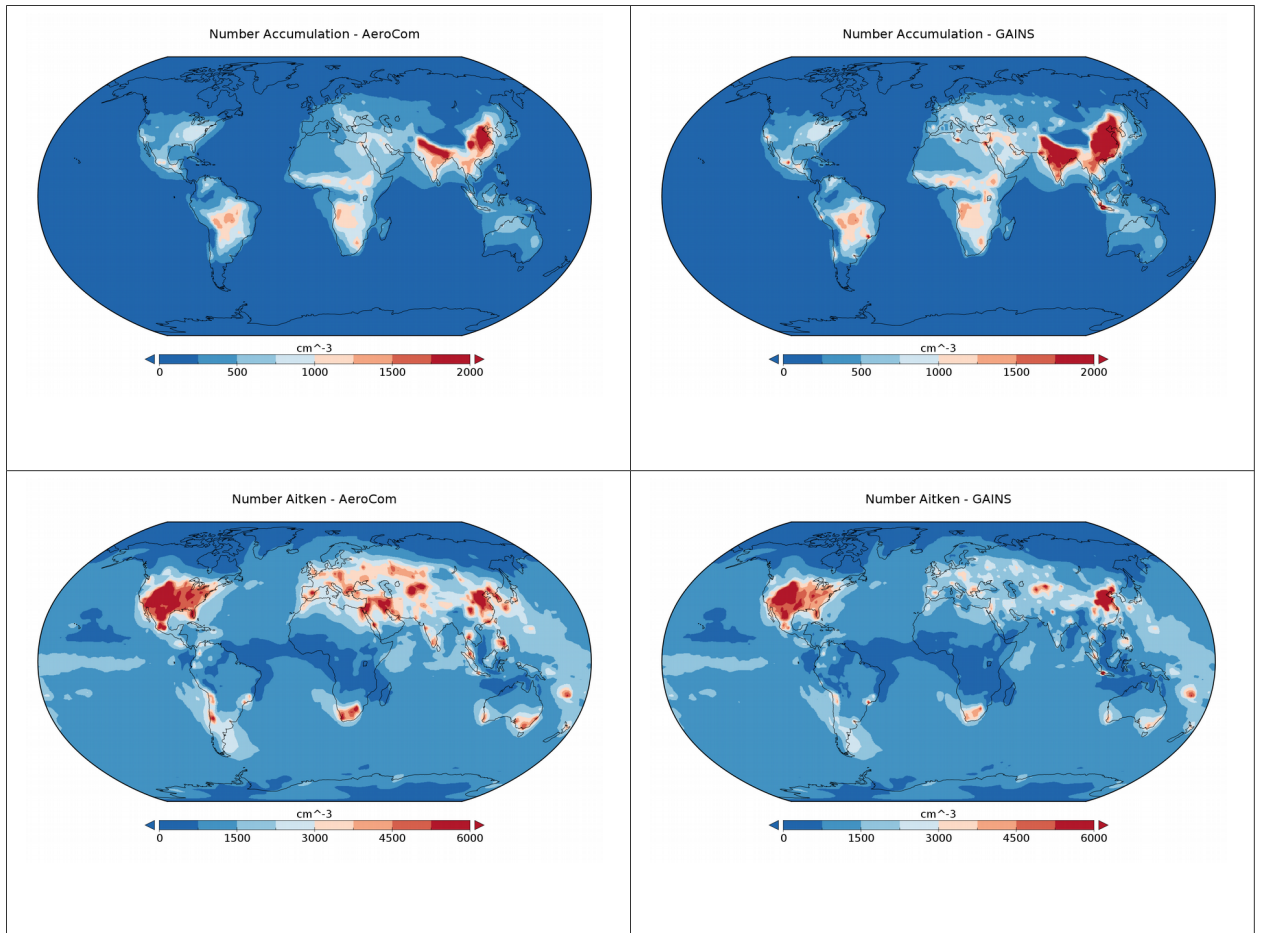


1145 Figure 4. Annual-averaged number of particles compared to observational data.
 1146 Measurement sites: 1: Botsalano; 2: Cabauw 3: Hohenpeissenberg; 4: Hyytiälä; 5: K-Pusztá;
 1147 6: Melpitz; 7: Nanjing; 8: Po Valley; 9: Sao Paulo; 10: Tomsk FNV; 11: Värriö. Both plots
 1148 include 1:1 and dashed 1:2, 2:1 lines.

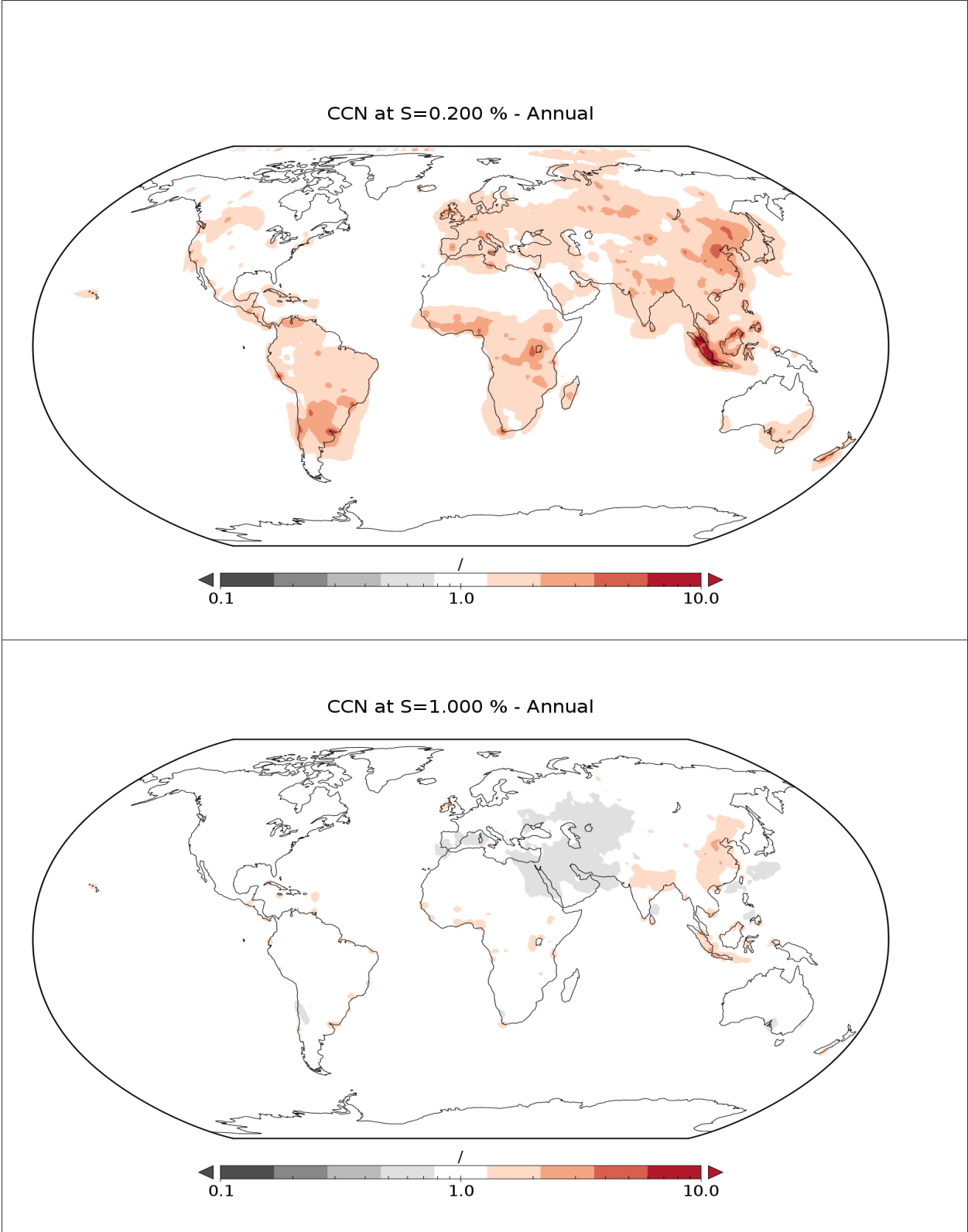


1149 Figure 5. Modeled particle number size distributions compared to observations at 6
 1150 measurement sites.

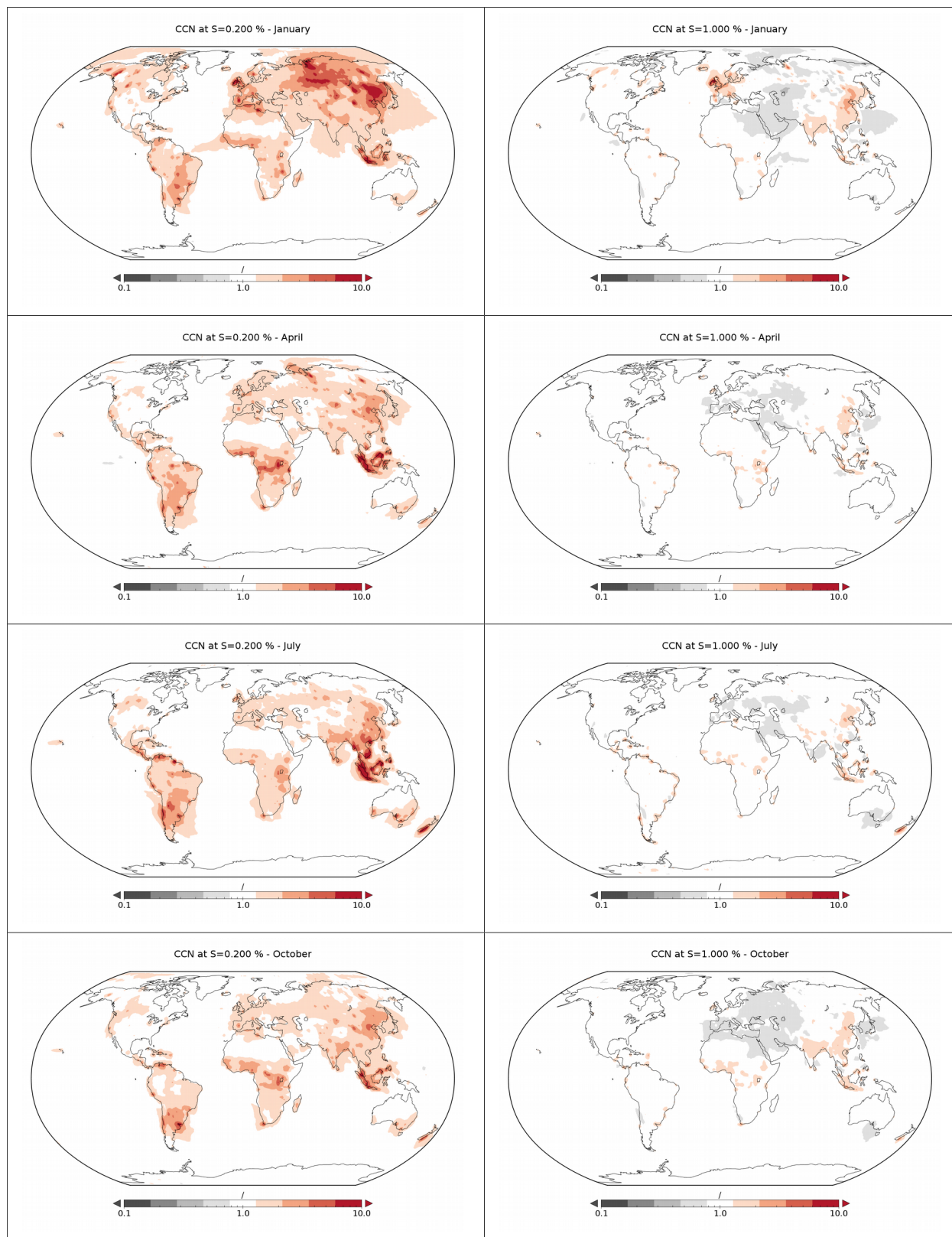
1151
 1152
 1153



1154 Figure 6. Modeled annual particle number concentrations for accumulation mode (top) and
 1155 Aitken mode (bottom), at surface level.
 1156
 1157
 1158
 1159
 1160
 1161
 1162
 1163
 1164
 1165
 1166
 1167
 1168
 1169
 1170
 1171
 1172
 1173
 1174



1175 Figure 7. Modeled annual GAINS/AeroCom ratios of CCN0.2 and CCN1.0, at surface level.



1176 Figure 8. Modeled seasonal GAINS/AeroCom ratios of CCN0.2 and CCN1.0, at surface level.